Published in final edited form as:

J Immunol. 2015 July 15; 195(2): 587–601. doi:10.4049/jimmunol.1402545.

Functional heterogeneity and anti-mycobacterial effects of mouse mucosal associated invariant T (MAIT) cells specific for riboflavin metabolites[1]

Isaac G. Sakala[1a,2,*], **Lars Kjer-Nielsen**[3], **Christopher S. Eickhoff**[1a], **Xiaoli Wang**[2], **Azra Blazevic**[1a], **Ligong Liu**[4,8], **David P. Fairlie**[4,8], **Jamie Rossjohn**[5,6,7], **James McCluskey**[3], **Daved H. Fremont**[2], **Ted H. Hansen**[2,*,‡], and **Daniel F. Hoft**[1a,1b,*,‡]

[1a]Department of Internal Medicine, Division of Infectious Diseases, Allergy & Immunology, Edward A. Doisy Research Center, Saint Louis University School of Medicine, 1100 S. Grand Blvd. Saint Louis, MO 63104, U.S.A

[1b]Department of Microbiology and Immunology, Edward A. Doisy Research Center, Saint Louis University School of Medicine, 1100 S. Grand Blvd. Saint Louis, MO 63104, U.S.A

[2]Department of Pathology and Immunology, Washington University School of Medicine, 660 S. Euclid Ave, Saint Louis, MO 63110, U.S.A

[3]Department of Microbiology and Immunology, Peter Doherty Institute for Infection and Immunity, The University of Melbourne, Parkville, VIC 3010, Australia

[4]Division of Chemistry and Structural Biology, Institute of Molecular Bioscience, The University of Queensland, Brisbane, QLD 4072, Australia

[5]Department of Biochemistry and Molecular Biology, School of Biomedical Sciences, Monash University, Melbourne, Clayton, VIC 3800 Australia

[6]Institute of Infection and Immunity, Cardiff University, School of Medicine, Heath Park, Cardiff CF14 4XN, UK

[7]Australian Research Council Centre of Excellence for Advanced Molecular Imaging, Monash University, Clayton, Victoria 3800, Australia

[8]ARC Centre of Excellence in Advanced Molecular Imaging, The University of Queensland, Brisbane, Queensland 4072, Australia

Abstract

Mucosal associated invariant T (MAIT) cells have a semi-invariant TCR Vα chain, and their optimal development is dependent upon commensal flora and expression of the non-polymorphic

[1]This work was supported by grants from National Institutes of Health (NIH: RO1-AI046553 to T.H.H and R01-A148391 to D.F.H) and the National Health and Medical Research Council of Australia (NHMRC: Senior Principal Research Fellowship to D.P.F, NHMRC Australia Fellowship to J.R and program grant 1016629 to J.R and J.M).

[*]Corresponding authors: Daniel F. Hoft, MD, Ph.D., Phone: 314-977-5500; Fax: 314-771-3816; hoftdf@slu.edu. Ted H. Hansen, Ph.D., hansen@pathology.wustl.edu. Isaac G. Sakala, Ph.D., Isaac.Sakala@gmail.com.
[‡]These co-senior authors contributed equally to this work

Disclosures

The authors have no financial conflict of interest.

MHC class I-like molecule MR1. MAIT cells are activated in an MR1-restricted manner by diverse strains of bacteria and yeast suggesting a widely shared Ag. Recently, human and mouse MR1 were found to bind bacterial riboflavin metabolites (ribityllumazines, RL Ag) capable of activating MAIT cells. Here we use MR1/RL tetramers to study MR1-dependency, subset heterogeneity and protective effector functions important for tuberculosis (TB) immunity. Although tetramer$^+$ cells were detected in both MR1$^{+/+}$ and MR1$^{-/-}$ TCR *Vα19i* transgenic (Tg) mice, MR1 expression resulted in significantly increased tetramer$^+$ cells co-expressing TCR Vβ6/8, NK1.1, CD44 and CD69, that displayed more robust *in vitro* responses to IL-12+IL-18 and RL Ag, indicating that MR1 is necessary for the optimal development of the classic murine MAIT cell memory/effector subset. In addition, tetramer$^+$ MAIT cells expressing CD4, CD8 or neither developing in MR1$^{+/+}$ *Vα19i* Tg mice had disparate cytokine profiles in response to RL Ag. Therefore, murine MAIT cells are considerably more heterogeneous than previously thought. Most notably, after mycobacterial pulmonary infection heterogeneous subsets of tetramer$^+$ *Vα19i* Tg MAIT cells expressing CXCR3 and α4β1 were recruited into the lungs and afforded early protection. In addition, *Vα19iCα*$^{-/-}$*MR*$^{+/+}$ mice were significantly better protected than *Vα19iCα*$^{-/-}$*MR1*$^{-/-}$, wild type and MR1$^{-/-}$ non-transgenic mice. Overall, we demonstrate considerable functional diversity of MAIT cell responses, and also that MR1-restricted MAIT cells are important for TB protective immunity.

Introduction

Mucosal associated invariant T (MAIT) cells, display a limited T cell receptor (TCR) repertoire and are restricted by the non-polymorphic major histocompatibility complex (MHC) class I-like molecule MR1 (1). Human and mouse MR1 were recently shown to bind riboflavin (vitamin B2) and folic acid (vitamin B9) metabolites, but only riboflavin metabolites activated MAIT cells *in vitro* (2–7). Accumulating evidence predicts that MAIT cells are relevant for the control of microbial infection. First, there is a striking evolutionary conservation in mammals of both the limited MAIT TCR usage and MR1 sequence, suggesting pathogen-driven purifying selection. More specifically, MAIT cells express structurally homologous invariant TCR alpha (iTCRα) chains consisting of the TRAV1-2 segment (Vα7.2*i* in humans) and TRAV1 (Vα19*i* in mice) joined mostly to a TRAJ33 (Jα33) segment resulting in a CDR3α of constant length (8). The Jα33-encoded CDR3α loop has three critical residues (Ser93α, Asn94α, Tyr95α) that engage both the α1 and α2 helices of MR1 (9). Of these, Tyr95α residue is the principal player in the invariant Jα33 use of the MAIT TCR, and is also conserved in non-TRAJ33 junctional genes namely TRAJ20 and TRAJ12, expressed by a minor subset of human MAIT cells (3, 4, 10–12). In addition the iTCRα of MAIT cells utilizes a broad TCR-β repertoire, but is preferentially paired with limited Vβ segments TRBV6 (Vβ13) or TRBV20 (Vβ2) in humans and TRBV19 (Vβ6) or TRBV13 (Vβ8.1 and Vβ8.2) in mice (4, 8, 13–15). Interestingly, most of the residues of the MAIT TCR α chain that contact MR1 are germ-line encoded, and the canonical CDR3α of MAIT cells is formed at a high frequency (3, 16). In addition, MR1 shares 80–98% amino acid sequence identity among mammals in its α1/α2 domains that interact with the MAIT TCR and/or antigenic riboflavin metabolites (3, 17). Thus the MR1/MAIT cell Ag presentation pathway has been strikingly conserved throughout mammalian evolution (18).

Vitamin B2 metabolites presented by MR1 appear to be the predominant antigens by which MAIT cells can detect a variety of microbes (2, 6). More specifically, Kjer-Nielsen et al. found that the vitamin B9 metabolite, 6-formylpterin (6-FP) bound human and mouse MR1 but did not stimulate MAIT cells. By contrast riboflavin intermediates including reduced 6-hydroxymethyl-8-D-ribityllumazine (rRL-6HM), 7-hydroxy-6-methyl-8-D-ribityllumazine (RL-6-Me-7-OH) and its precursor, 6,7-dimethyl-8-D-ribityllumazine (RL-6,7-diMe) stimulated MAIT cells in an MR1-dependent manner. Structural studies have shown that the form of Ag trapped by MR1 includes the relatively unstable adducts, 5-(2-oxoethylideneamino)-6-D-ribitylaminouracil (5-OE-RU) and 5- (2-oxopropylideneamino)-6-D-ribitylaminouracil (5-OP-RU), formed by the reaction between 5-amino-6-D-ribitylaminouracil and glyoxal or methylglyoxal respectively (6). MR1 tetramers formed between MR1 and either synthetic preparation of rRL-6HM or 5-OP-RU give identical results (6).

Evidence that vitamin B2 metabolites are predominant MAIT cell antigens includes the observation that the diverse bacterial and yeast strains previously shown to activate MAIT cells *in vitro* have a vitamin B2 synthesis pathway, whereas microbes previously shown to not activate MAIT cells lack this synthesis pathway (19, 20). Expansion in response to commensal flora antigens explains why MAIT cells are abundant in mucosal tissues. Furthermore, human liver is also constantly exposed to bacterial products absorbed from the gut, likely explaining why MAIT cells can constitute as high as 45% of the total lymphocytes in human liver (21–23). In addition MAIT cells represent up to 10% of the mature $CD8^+$ and/or DN T cells in the blood of healthy individuals (8, 22).

Further supporting their anti-microbial activity, following *in vitro* TCR ligation, MAIT cells rapidly secrete the inflammatory cytokines IFN-γ, TNFα and IL-17 (24, 25). In addition MAIT cells express chemokine receptors indicating their migratory potential and MAIT cell distribution is altered in several diseases (22). For example, patients infected with mycobacteria had increased numbers of MAIT cells in their infected lung and fewer MAIT cells in the blood, compared to uninfected controls (19, 20, 26). In addition, sharp and nonreversible decreases in MAIT cells were found in the blood and tissues of patients with HIV mono-infection and HIV/TB co-infection (27–30). It was speculated that this loss of MAIT cells was caused by HIV infection inducing MAIT cell exhaustion from exposure to bacterial products; and that loss of MAIT cells rendered HIV patients susceptible to opportunistic infections. MAIT cells have also been implicated in other diseases secondarily affected by microbiota imbalance such as multiple sclerosis, type 2 diabetes and inflammatory bowel disease (31–34).

As a foundation for future studies of the clinical relevance of MAIT cells, genetically defined mouse models continue to provide key insights into the development and antimicrobial mechanism of MAIT cells. For example, MR1 knockout mice were used in a seminal report to show that MAIT cell optimal development is dependent on MR1 expression (35). In addition $MR1^{-/-}$ mice were found to be more susceptible than wild type mice to bacterial infection, providing the first *in vivo* evidence that MAIT cells control bacterial infection (20, 24, 36, 37). Due to the paucity of MAIT cells in laboratory mouse strains compared with human, three different groups have reported the production of Vα19i

transgenic (Tg) mice. (13, 25, 38). These *Vα19i* Tg mice recapitulate several features of the phenotypic heterogeneity of human MAIT cells. For example, *Vα19i* Tg MAIT cells, like human MAIT cells include $CD8^+$($CD8\alpha\alpha$), $CD4^+$ and $CD4^-CD8^-$ (double negative, DN) subsets although in different proportions (13, 28, 39). In addition, subsets of both *Vα19i* Tg mouse MAIT cells and human MAIT cells express a similar NK receptor (NK1.1 in mouse and CD161 in humans). Furthermore, like human MAIT cells, mouse *Vα19i* Tg MAIT cells use diverse Vβ chains in addition to the ones that are preferred (4, 19). These similarities in the phenotypic heterogeneity of human and *Vα19i* Tg MAIT cells raise the largely unanswered question of the functional importance of different MAIT cell subsets.

In our initial mouse study we showed that MR1-restricted MAIT cells confer early protection against intranasal *Mycobacterium bovis* infection, providing *in vivo* evidence that MAIT cells are critical for the prompt control of mycobacterial infection (24). In the current study, we used Ag-loaded native mouse MR1 tetramers to investigate the subsets of MAIT cells important for anti-mycobacterial immunity, and gain insight into the mechanisms by which they mediate early protection against mycobacterial infection. We demonstrate that MR1/RL $tetramer^+$ mouse MAIT cells contain heterogeneous populations, and that MR1 expression leads to the development of more “classic” MAIT cell populations (increased $V\beta6/8^+$, $NK1.1^+$ MAIT cells which can be activated by either MR1-restricted TCR signaling or innate cytokine stimulation). We further show that these classical MR1-restricted MAIT cells are capable of providing important *in vivo* anti-mycobacterial effects.

Materials and Methods

Mice

The *Vα19i* Tg TCRα chain deficient ($C\alpha^{-/-}$) mice used in this study (on C57BL/6 [B6] genetic background) have been described before (25). The *Vα19i* Tg B6 MR1-sufficient mice ($MR1^{+/+}$) were crossed with $C\alpha^{-/-}$ B6 mice (B6.129S2-*Tcra*^{tm1Mom}/J; The Jackson Laboratory) to eliminate expression of endogenous TCRα chains to generate *Vα19iCα*$^{-/-}$*MR1*$^{+/+}$ mice. These *Vα19iCα*$^{-/-}$ Tg mice were further crossed with B6-$MR1^{-/-}$ mice to generate *Vα19iCα*$^{-/-}$*MR1*$^{-/-}$ mice (25). Therefore, the *Vα19i* Tg MR1 sufficient and deficient mice we used in all of our experiments exclusively express a Vα19i transgene that is the canonical TCR Vα of mouse MAIT cells. As previously described, MAIT cells isolated from these Tg mice utilize endogenous heterogeneous TCR Vβ chains, and thus *Vα19i* Tg T cells have characteristics of polyclonal MAIT cells (25). Inbred B6-$MR1^{-/-}$, *Vα19iCα*$^{-/-}$*MR1*$^{+/+}$ and *Vα19iCα*$^{-/-}$*MR1*$^{-/-}$ mice were a generous gift from Dr. Susan Gilfillan to Dr. Ted H. Hansen (Washington University, St. Louis, MO). B6.129P2-*H2-Kb*^{tm1} *H2-Db*^{tm1} N12 (H2-$K^{b-/-}$ H2-$D^{b-/-}$, homozygous H2-K^b H2-D^b double knockout) mice were a generous gift from Dr. Wayne Yokoyama (Washington University, St. Louis, MO). H2-$K^{b-/-}$ H2-$D^{b-/-}$ mice are virtually devoid of Class Ia cell surface molecules (40). Wild type B6 mice (B6-WT) were purchased from The Jackson Laboratory. This animal study was performed in strict compliance with the recommendations in the Guide for the Care and Use of Laboratory Animals of the National Institutes of Health, Office of Laboratory Animal Welfare. Mice were bred and maintained under specific-pathogen-free conditions, and experimental procedures used as described in the study protocol were

approved by the Washington University's Institutional Animal Care and Use Committee, the Animal Studies Committee and the Saint Louis University Animal Care and Use Committee.

Purification of splenic Vα19i Tg T cells, conventional CD4$^+$, CD8$^+$ T cells, innate type I NKT and NK cells

Single-cell suspensions were prepared from spleens aseptically removed from naïve mice. After red blood cells were lysed with ammonium chloride buffer, *Vα19i* Tg T-cells, CD4$^+$, CD8$^+$ T cells and NK cells were purified by negative selection using immunomagnetic isolation kits (Miltenyi Biotec) following the manufacturer's instructions. The isolation of iNKT cells was performed in a two-step procedure. First, the non-NK1.1$^+$ iNKT cells were labelled with a cocktail of biotin-conjugated antibodies and subsequently depleted by separation over a MACS column. In the second step, the NK1.1$^+$ iNKT cells were positively isolated with anti-NK1.1-allophycocyanin and anti-allophycocyanin Microbeads. The purity was checked by flow cytometry and was consistently greater than 98%.

Isolation of liver T lymphocytes by cation chelator-containing buffer

Liver T lymphocytes were isolated by perfusion with 10mM EDTA/PBS according to the protocol described by Fang and colleagues (41). Briefly, 100μl of 14.8 mg/ml sodium pentobarbital (75 mg/kg final dosage) and 3–5μl Heparin Sodium Injection were injected via the intraperitoneal route. Once the mouse was unconscious, the abdomen and thorax were rapidly opened to expose the superior vein cava. The superior vein cava was carefully tied using A184 surgical suture. Both right and left kidney renal veins were carefully tied. With the intestines reflected to the mouse's left, a 23G scalp vein set (BD 367285) was carefully inserted into the portal vein and the scalp vein set held in place with an artery clamp (Bulldog Serrefines, F.S.T Item # 18050–28). Through the mouse hind fat tissue, the inferior vena cava was cannulated with an 18 G needle. The liver was first perfused with 10 ml PBS with $CaCl_2$ and $MgCl_2$ via the scalp vein set and the flow out blood collected with a 100 mm petri dish under the 18 G needle. Intrahepatic T cells were isolated by perfusion with 20 ml 10 mM EDTA/PBS without $CaCl_2$ and $MgCl_2$. This second flow out was collected and transferred into 50 ml centrifuge tube and centrifuge for 5 minutes at 400 g. The cell pellet was resuspended with the 1 ml ACK Lysis buffer to lyse red blood cells. Cells were then washed with DMEM supplemented with 10% FBS and counted.

Preparation of murine bone marrow-derived macrophages (BMDMϕ)

Bone marrow cells isolated from femora of B6-WT, B6-MR1$^{-/-}$ and B6- H2-K$^{b-/-}$ H2-D$^{b-/-}$ mice were cultured (2.5×10^4 cells/well) in 10% fetal bovine serum (FBS) DMEM medium with 20ng/ml murine recombinant M-CSF (PeproTech) for 7 days. After 7 days culturing, BMDMφ formed a confluent monolayer with estimated density of 2.5×10^5 cells per well.

IFN-γ response to IL-12/IL-18 cytokines

Purified naïve T cells were cultured in 96-well plates (2 x 10^5/well) alone or stimulated with recombinant murine IL-12 (500pg/ml: PeproTech) and/or IL-18 (5pg/ml – 1000pg/ml; R&D systems) for 24h at 37°C. IFN-γ levels in the supernatants of triplicate cultures were

determined using a sandwich ELISA kit (R&D Systems). For intracellular IFN-γ response, cells were pre-stimulated as described above for 16–20h before addition of 10μg/ml brefeldin A solution (Sigma-Aldrich) and further incubated for 4h (intracellular protein accumulation period). For PMA plus ionomycin stimulation condition, brefeldin A solution and PMA (0.05μg/ml final) plus ionomycin (0.75 μg/ml final) were added simultaneously and T cells incubated for 4h. Cells from triplicate wells were pooled, washed and stained with LIVE/DEAD® Fixable Aqua Dead Cell dye (Life Technologies) for 30 min at 4°C. Subsequently cells were surface stained with fluorochrome-conjugated anti-mouse CD3ε, CD4, CD8α and Vβ6/8.1–2 for 30 min at 4°C then were treated with Cytofix/Cytoperm (BD Biosciences) and stained with anti-mouse IFN-γ-PE (BD Pharmingen). Data were acquired on BD LSR II flow cytometer and analyzed using FlowJo analysis software.

Vitamin B2 metabolites

Activating and non-activating synthetic vitamin B metabolites were described previously (2, 6). In this study we used synthetic rRL-6HM to make first generation (1G) MR1/RL tetramers and to stimulate MAIT cells *in vitro,* and 5-OP-RU as the stimulatory vitamin B2 metabolite to make second generation (2G) MR1/RL tetramers.

Generation of MR1(K43A)–rRL-6HM (1G) and MR1(wild type)–5-OP-RU (2G) tetramers to detect MAIT cells

The generation of MR1(K43A) tetramers, loaded with synthetic rRL-6HM, and wild type MR1 tetramers, loaded with 5-OP-RU has been previously described (4, 6). Briefly, refolded and purified empty carboxy-terminal cysteine-tagged-MR1(K43A) was loaded with a 136 molar excess of synthetic rRL-6HM for 4 h at room temperature in the dark. Cysteine-tagged wild-type MR1–5-OP-RU was reduced with 5 mM DTT for 20 min before buffer exchange into PBS using a PD-10 column (GE Healthcare). Negative control MR1 tetramers were MR1(K43A)–empty tetramers (for 1G) and MR1(wild type) loaded with the non-stimulatory 6-FP (for 2G). MR1(K43A)-empty, MR1(K43A)–rRL-6HM, MR1(wild type)–6-FP or MR1(wild type)–5-OP-RU were then biotinylated with Maleimide-PEG2 biotin (Thermo Scientific) with a 30:1 molar ratio of biotin-to-protein at 4 °C for 16 h in the dark. Biotinylated MR1 was subjected to S200 10/300 GL (GE Healthcare) chromatography to remove excess biotin. Biotinylated monomers were tetramerized with streptavidin conjugated to PE (SA-PE) (BD Pharmingen).

MAIT cell activation by the soluble rRL-6HM vitamin B2 metabolite

Prior to co-culture, CH27-mMR1 cells, a mouse B cell lymphoma transduced to overexpress mouse MR1 (42–44), were pre-incubated with either medium (no antibody control), 10μg/ml anti-MR1 blocking antibodies (clones 26.5 and 8F2.F9) for 1h at 37°C. These CH27-mMR1 cells were then co-cultured with sorted tetramer^{+} *Vα19i* Tg T cells in 96-well plates (Corning Inc.) at APC:T cell ratio of 1:5 along with synthetic vitamin B2 metabolite, rRL-6HM (76.2 μM final concentration) for 60h at 37°C in the absence or presence of 10μg/ml anti-MR1 blocking antibodies. MAIT cell activation was determined by using Milliplex MAP mouse cytokine / chemokine panel I and CD8^{+} T cell assay kits (EMD Millipore).

MR1/RL tetramer staining and flow cytometry

Approximately 1 x 10^6 T cells were washed with cold FACS staining buffer (1x PBS with 2% FBS) and stained with either: PE-conjugated control unloaded (empty) mouse MR1(K43A) tetramer or PE-conjugated rRL-6HM-loaded mouse MR1(K43A) tetramer at 20 μg/ml (1G tetramers; (4)); or PE-conjugated non-stimulatory control mouse MR1(wild type)–6-FP tetramer or PE-conjugated mouse MR1(wild type)–5-OP-RU tetramer at 1.4 μg/ml (2G tetramers; (6)) for 45 minutes at room temperature in the dark. Immediately thereafter, cells were co-stained for 30 minutes on ice with mixture of selected fluorochrome-conjugated antibodies including anti-mouse CD3-Pacific blue (BD Biosciences), CD4-PerCP or Alexa Fluor 700 (BioLegend), CD8α-APC-H7 (BD Biosciences), CD8β-Alexa Fluor 647 or PerCP-Cy5.5 (BioLegend), NK1.1-PerCP-Cy5.5 or -BV510 (clone PK136, BD Biosciences), CD69-APC, CD44-PE-Cy7, Vβ6/Vβ8.1–8.2 TCR-FITC (BD Biosciences), CXCR3-PE-Cy7 and α4β1 integrin-Alexa Fluor 647 (BioLegend). After washing once with 2 ml of FACS staining buffer, data was acquired on BD FACS CantoII, BD LSR II or BD FACSAria flow cytometers and analyzed using FlowJo analysis software (Tree Star).

Mycobacteria

Mycobacterium bovis TMC 1010 (ATCC 35733; BCG Danish) and *M. tuberculosis* strain Erdman (BEI Resources-NR-15404 or ATCC 35801) were grown in Middlebrook 7H9 broth (BD Difco™) supplemented with 10% oleic acid-albumin, dextrose and catalase enrichment (OADC) and 0.05% Tween 80. When the bacterial density reached log-phase growth, mycobacteria were harvested and stored in PBS at −80°C. The concentration (CFU/ml) was quantified on Middlebrook 7H10 agar (BD Difco™) plates. Before being used for infection, bacteria were thawed and sonicated to obtain a single-cell suspension, and diluted appropriately in antibiotic-free complete RPMI-1640 medium.

In vivo mycobacterial infection

Eight (8) – 10 week old B6-$MR1^{-/-}$, B6-WT, $Va19iCa^{-/-}MR1^{-/-}$ and $Va19iCa^{-/-}MR1^{+/+}$ mice were infected with BCG Danish via the intranasal route. Groups of 5 mice were inoculated with 10^7 CFU/mouse of the BCG Danish suspension in 50μl (25ul/nostril) under anesthesia. On day 10 post-infection, mice were euthanized and peripheral blood, bronchoalveolar lavage (BAL) cells, and lungs were collected. The collected total BAL cells were enumerated by trypan blue staining technique. The frequency of tetramer-reactive T cells in BAL and peripheral blood were determined by FACS as described above. In the aerosol infection, *M. tuberculosis* strain Erdman was diluted to 10^7 CFU/ml in PBS with 0.04% Tween 80. A nebulizer (CH Technologies, Westwood, NJ) was set to liquid feed at 1 ml/min and airflow at 1 liter/min to expose B6-WT or $Va19iCa^{-/-}MR1^{+/+}$ mice to *M. tuberculosis* Erdman. A 20 min exposure to the aerosol resulted in the delivery of 100 to 300 infectious bacilli per mouse lung. Mycobacterial load was determined in lung homogenates on Middlebrook 7H10 agar plates supplemented with 10% OADC as previously described (24).

Activation of MR1$^{-/-}$ Vα19i Tg T cells by MHC-class Ia-restricted epitopes

B6-WT, B6-MR1$^{-/-}$ and B6- H2-K$^{b-/-}$ H2-D$^{b-/-}$ BMDMφ, prepared as described above, were infected with BCG Danish at a multiplicity of infection (MOI) of 3:1 (bacteria to macrophage) in antibiotic free 10% FBS DMEM medium at 37°C in 5% CO_2. After overnight culture, infected BMDMφ were washed with 10% FBS DMEM medium to remove the extracellular BCG before co-culture with purified *Vα19iCα*$^{-/-}$*MR1*$^{-/-}$CD8$^+$ T cells or total Tg T cells at the ratio of 1:1. Activation of *Vα19iCα*$^{-/-}$*MR1*$^{-/-}$ CD8$^+$ T cells was assessed by intracellular IFN-γ and MIP-1α production after overnight (24h) co-culture at 37°C in 5% CO_2. Inhibition of intracellular BCG growth in BMDMφ by purified total T cells as a measure of their function was determined at the end of 72h co-culture. Co-cultured cells were lysed with 0.2% saponin to release intracellular BCG. Mycobacteria were radiolabeled with tritiated uridine, as previously described (24, 45), to determine the viability of bacteria in B6-WT, B6-MR1$^{-/-}$ and B6- H2-K$^{b-/-}$ H2-D$^{b-/-}$ macrophages. Briefly, [5,6-3H]uridine (Perkin Elmer, Waltham, MA) at 1 μCi/ml prepared in Middlebrook 7H9 broth supplemented with 10% ADC enrichment medium (BD BBL 211887; Becton, Dickinson, Franklin Lakes, NJ) was added to saponin lysates. After incubation at 37°C for 72 h, the tritiated uridine-pulsed mycobacteria were harvested (Tomtec Harvester 96 MACH III M; Tomtec, Hamden, CT) onto glass fiber filters (Perkin Elmer, Waltham, MA), and radioactivity was quantitated by liquid scintillation counting (Wallac MicroBeta TriLux 1450; Perkin Elmer, Waltham, MA). The percentages of BCG growth inhibition were calculated by the following formula: percent inhibition 100 – [100 X (disintegrations per minute from T cell-infected Mφ co-cultured wells/disintegrations per minute from infected Mφ alone wells)].

Statistical analysis

Statistical analyses of experimental data were performed using GraphPad Prism (GraphPad Software, San Diego, CA). For comparisons, unpaired 2-tailed *t* test with Welch's correction, Mann-Whitney U and 2way ANOVA tests were applied.

Results

Phenotypic characterization of MR1/RL tetramer$^+$ T cells in uninfected Vα19i Tg mice on both MR1$^{+/+}$ and MR1$^{-/-}$ genetic backgrounds

Due to low frequency of MAIT cells in standard laboratory strains of mice and the lack of specific antibodies to the mouse Vα19i chain, identification of mouse MAIT cells in wild type mice has been extremely difficult. *Vα19i* Tg mice were previously shown to have increased frequency of MAIT cells as determined by the biased Vβ6 or Vβ8.1/8.2 (Vβ6/8) chain usage in *Vα19iCα*$^{-/-}$*MR1*$^{+/+}$ mice (25). However, Vβ6/8 chains can pair with the Vα19i chain in *Vα19iCα*$^{-/-}$*MR1*$^{-/-}$ mice and the Vα19i chain can pair with other Vβ chains in Tg mice, obscuring identification of the classically described MR1-dependent MAIT cells. Furthermore, NK cell activation markers (e.g.-NK1.1 in the mouse and CD161 in humans) have been associated with classic MAIT cell populations, but whether expression of these NK markers can identify the functionally important MAIT cell lineage or simply indicate the previous activation status of peripheral MAIT cells remains unknown. The availability of mouse MR1/RL tetramers offers for the first time an approach to detect

MAIT cells based on their RL-specific TCR and determine how this Ag specificity relates to Vβ6/8 and NK1.1 expression and MAIT cell functional responses.

Using first generation (1G) MR1/RL tetramers in which MR1 K43A mutated molecules were loaded with or without the vitamin B2 metabolite rRL-6HM, 16.3 ± 1.6% and 4.5 ± 1.0% of splenic CD3$^+$ T cells from *Vα19iCα*$^{-/-}$*MR1*$^{+/+}$ and *Vα19iCα*$^{-/-}$*MR1*$^{-/-}$ mice, respectively, were stained by RL-loaded MR1 tetramers but not by RL-empty tetramers (Fig. 1A and 1C-top panel). These results indicated that mouse MR1/RL tetramer can specifically detect MR1/RL-reactive T cells in the *Vα19i* TCR Tg mouse. To further characterize phenotypically and functionally MR1/RL-reactive cells, and to understand the requirements for MR1 and CD4/CD8 co-receptors in the development of mouse MAIT cells, a more stable MR1/RL tetramer (second generation, 2G) was used in the current study (6). We used the gating strategy shown in Suppl. Fig. 1A and 1B to analyze lymphocyte population for the frequency and phenotype of tetramer$^+$ CD3$^+$ T cells in the thymus, two secondary lymphoid organs (mesenteric lymph nodes [mLN] and spleen), blood and liver peripheral organ. Similar to what was observed with the empty 1G tetramer, the negative control 2G tetramers loaded with non-antigenic 6-FP stained less than 1% of CD3$^+$ splenocytes from both *Vα19iCα*$^{-/-}$*MR1*$^{+/+}$ and *Vα19iCα*$^{-/-}$*MR1*$^{-/-}$ mice. However, the 2G tetramer loaded with antigenic 5-OP-RU stained a markedly higher percentage of splenic CD3$^+$ T cells (50.2 ± 0.5% in *Vα19iCα*$^{-/-}$*MR1*$^{+/+}$ mice and 32.0 ± 0.6% in *Vα19iCα*$^{-/-}$*MR1*$^{-/-}$) (Fig. 1B and 1C-bottom panel). Thus, the 2G tetramers were more sensitive while retaining antigenic specificity. Of note, although a higher proportion of tetramer$^+$ splenic T cells was detected in *Vα19iCα*$^{-/-}$*MR1*$^{-/-}$ mice with the 2G tetramers than with the 1G tetramers, both the percentages and numbers stained were significantly lower than what was detected in *Vα19iCα*$^{-/-}$*MR1*$^{+/+}$ mice (Fig. 1C-bottom panel). Tetramer$^+$ MAIT cells were also detected in the thymus, mLN, peripheral blood and the liver, and ranged from the lowest percentage (45 ± 1.2%) among mature (CD3^{high}) thymocytes to the highest frequency (60 ± 1.9%) in the liver of *Vα19i* Tg MR1 sufficient mice (Suppl. Fig. 1B-left dot plots column and 1C-top panel). In contrast, in *Vα19i* Tg MR1 deficient mice, we observed a gradual decrease in the proportion of tetramer$^+$ cells comparing thymocytes and liver peripheral tissue (Suppl. Fig. 1C-top panel). Furthermore, the proportions of tetramer$^+$ cells were significantly lower in all tissues of MR1 deficient Tg mice compared with MR1 sufficient Tg mice. Most impressively, the diminution in proportion of liver tetramer$^+$ CD3$^+$ T cells was 56% less compared with that in *Vα19iCα*$^{-/-}$*MR1*$^{+/+}$ mice. Therefore, our results are consistent with the previous findings that optimal peripheral development/expansion of MAIT cells depends on MR1 expression. Further demonstrating the specificity of the 2G tetramers, neither purified NK nor type I NKT cells were stained (Fig. 1D). A less than 5% staining of type I NKT cells is an acceptable background because the negative control MR1 6-FP tetramer similarly stained <5% of these cells, demonstrating non-specific low level staining. Also, consistent with the known low frequency of MAIT cells in specific-pathogen free laboratory mice, the proportion of splenic T cells reactive with 2G MR1/RL tetramers was not different from the control MR1 6-FP tetramer stained cells compared with *Vα19iCα*$^{-/-}$*MR1*$^{+/+}$ T cells (Fig. 1D). These data demonstrate that the tetramer staining of *Vα19i* Tg T cells is not attributable to non-specific binding by the MR1/RL-tetramers. Thus, the specificity and increased

sensitivity of 2G tetramers provides the unique potential for defining the phenotypic, developmental and functional heterogeneity of MAIT cell subsets in *Vα19i* Tg mice, including RL-reactive T cells that develop in the absence of MR1.

As Vβ6 and Vβ8 are the major Vβ chains previously found to pair with Vα19i, we next analyzed expression of Vβ6/8 in tetramer$^+$ MAIT cells. In the thymus, mLN, spleen and peripheral blood of *Vα19iCα*$^{-/-}$*MR1*$^{+/+}$ mice, approximately 31–42% of tetramer$^+$ T cells co-expressed Vβ6/8 compared with 25–28% in *Vα19iCα*$^{-/-}$*MR1*$^{-/-}$ mice (Suppl. Fig. 1B-middle dot plots column; 1C-middle panel and Fig. 1E, 1F). A relatively higher level of Vβ6/8 expression on tetramer$^+$ CD3$^+$ T cells developing in the presence of MR1 was seen in the liver (53 ± 3.1%) (Suppl. Fig. 1B-middle dot plots column and 1C-middle panel). Vβ6/8 expression on liver tetramer$^+$ MAIT cells was 1.7-fold higher than on tetramer$^+$ mature thymocytes, and there was also 3-fold reduction in Vβ6/8 pairing (17 ± 0.9%) in the liver tetramer$^+$ T cells in *Vα19iCα*$^{-/-}$*MR1*$^{-/-}$ mice. We also compared Vβ6/8 pairing in immature (CD3_CD4$^+$CD8$^+$ and CD3$^{low/intermediate}$CD4$^+$CD8$^+$) versus mature (CD3^{high}) thymocytes (46) in the two *Vα19i* Tg mice strains. The level of Vβ6/8 expression was very low (<2%) on both subsets of immature thymocytes (data not shown). However, marked increases in Vβ6/8 expression were seen on mature thymocytes. In *Vα19iCα*$^{-/-}$*MR1*$^{+/+}$ mice, 31 ± 0.7% of tetramer$^+$ mature thymocytes expressed Vβ6/8 compared with 25 ± 0.5% in *Vα19iCα*$^{-/-}$*MR1*$^{-/-}$ mice (Suppl. Fig. 1C-middle panel). Similar differences in Vβ6/8 co-expression by tetramer$^+$ T cells were seen comparing CD4$^+$, DN and CD8$^+$ subsets in *Vα19i* Tg MR1 sufficient and deficient mice (data not shown).

In addition, we determined NK1.1 expression on tetramer$^+$ CD3$^+$ cells in the thymus, mLN, spleen, peripheral blood and liver tissue. In MR1$^{+/+}$ and MR1$^{-/-}$ *Vα19i* Tg mice, the level of NK1.1 expression was similar (<3%) on tetramer$^+$ mature thymocytes, but progressively increased in secondary lymphoid organs, blood and liver (Suppl. Fig. 1B-right dot plots column, 1C-bottom panel and Fig. 1E, 1F-right panels). This steady increase in proportions of NK1.1$^+$ tetramer$^+$ T cells from the most naïve to most peripherally expanded/activated populations was most remarkable in MR1 sufficient Tg mice. In these mice, the liver contained 63 ± 4.9% of NK1.1$^+$ tetramer$^+$ cells, followed by blood (48 ± 1.4%), spleen (18 ± 1.9%), mLN (11 ± 1.1%). It is important to point out that large fractions of CD3$^+$ tetramer$^+$ T cells in all tissues were both Vβ6/8$^-$ and NK1.1$^-$. These results indicate that as we and others recently reported for human MAIT cells (4, 47); murine MAIT cells as defined by MR1/RL tetramer staining, are considerably more heterogeneous than previously thought. Nonetheless, our data do confirm that the classical murine Vβ6/8$^+$, NK1.1$^+$ MAIT cells are dependent on MR1 for optimal development.

To identify CD4$^+$, CD8$^+$ and DN subsets of splenic MR1/RL-reactive MAIT cells in uninfected control mice, we used the gating strategy shown in Fig. 2A and 2B. Representative plots in Fig. 2A show the gating of splenic CD3$^+$ T subsets, and indicate that the fraction of *Vα19i* Tg T cells that express neither CD4 nor CD8 co-receptors represent ~50–55% of total CD3$^+$ T cells. As previously shown by the Gilfillan lab (25), most mature CD3$^+$ T cells in both MR1$^{+/+}$ and MR1$^{-/-}$ *Vα19i* Tg mice are DN subset. This was not unexpected because of decreased thymic DN-to-CD4/CD8 double positive developmental transition seen in most TCR Tg mouse systems due to early expression of TCRα-chain (48,

49). Despite this limitation, the expressed TCRα chain can pair with a diverse repertoire of endogenous TCR β chains for cell surface expression (49). The 2G MR1/RL tetramers stain ~50% of these total T cells, indicating that about half of splenic DN *Vα19i* Tg T cells are RL-reactive MAIT cells. These data may suggest that while the vitamin B2 metabolites are the predominant antigens, there may be other MAIT cell ligand(s) yet to be discovered. In *Vα19iCα*$^{-/-}$*MR1*$^{+/+}$ mice, the 2G MR1/RL tetramers stained the following percentages of CD3$^+$ T cell subsets: 43 – 50% in the thymus, 47 – 56% in secondary lymphoid tissues/ blood and 54 – 62% in the liver peripheral organ (Fig. 2C). We found that the proportions of tetramer$^+$ cells were higher in *Vα19iCα*$^{-/-}$*MR1*$^{+/+}$ mice than in *Vα19iCα*$^{-/-}$*MR1*$^{-/-}$ mice in all CD3$^+$ T cell subsets, except thymic CD8$^+$ T cells (Fig. 2C). Most remarkably, tetramer$^+$ DN T cells were reduced in *Vα19iCα*$^{-/-}$*MR1*$^{-/-}$ mice (Fig. 2C and 2D). These data indicate that MR1 is important for optimal development of all MAIT cell co-receptor subsets, but has the biggest impact on the development of the DN subset of tetramer$^+$ MAIT cells. Tetramer$^+$ T cells in the tested tissues in *Vα19iCα*$^{-/-}$*MR1*$^{+/+}$ mice were mainly DN with fewer CD4$^+$ and CD8$^+$ cells (Fig. 2D, top pie charts). This relative distribution of MR1/RL-reactive MAIT cell co-receptor expression is similar to that previously reported by Gilfillan et al. identifying MAIT cells based on biased Vβ6/8 expression in *Vα19iCα*$^{-/-}$*MR1*$^{+/+}$ mice (25). Interestingly, we found an increase in relative frequency of the tetramer$^+$ CD8$^+$ subset in *Vα19i* Tg MAIT cells developing in the absence of MR1 (Fig. 2D, bottom pie charts), suggesting the possibility that in the absence of MR1, MR1/RL-reactive cells can be selected/expanded by interacting with classical MHC-Ia molecules.

Innate functions of tetramer$^+$ T cells in Vα19iCα$^{-/-}$MR1$^{+/+}$ and Vα19iCα$^{-/-}$MR1$^{-/-}$ mice

A pivotal function of MAIT cells is their ability to rapidly release cytokines in response to innate stimuli. We and others have reported that mouse and human MAIT cells can respond to IL–12 and IL-12 plus IL-18 in a TCR-independent manner (24, 50). Here we extend these findings to investigate Ag presenting cell (APC)- and MR1-dependence of these innate cytokine responses of MAIT cells. After IL-12 treatment, *Vα19i* Tg T cells cultured with or without uninfected BMDMφ secreted comparable amounts of IFN-γ. However, *Vα19i* Tg T cells that developed in MR1 expressing mice secreted significantly higher levels of IFN-γ than *Vα19i* Tg T cells from MR1 deficient mice (representative experiment shown in Fig. 3A-i). We next extended these findings to test the response of *Vα19i* Tg T cells to IL-12 plus IL18, known to synergistically enhance IFN-γ responses of NK and type I NKT cells (51, 52). IFN-γ was not induced in *Vα19i* Tg T cells from MR1 sufficient mice following stimulation with IL-18 alone (data not shown), whereas the combined stimulation with 500 pg/ml of IL-12 resulted in strikingly higher levels of IFN-γ production (Fig. 3A-ii); and as previously reported, anti-MR1 blocking mAb did not inhibit these innate responses (24, 50). Of note the responses of *Vα19iCα*$^{-/-}$*MR1*$^{+/+}$ T cells to IL-12 plus IL-18 were comparable to the responses of splenic NK and type I NKT cells purified from wild type B6 mice (Fig. 3A-ii). In contrast, purified splenic CD4$^+$ or CD8$^+$ T cells from B6 mice secreted very low levels of IFN-γ after IL-12 plus IL-18 treatment. Interestingly, *Vα19i* Tg T cells from MR1 knockout mice responded to IL-12 plus IL-18 significantly better than conventional CD4$^+$ and CD8$^+$ T cells; however the responses to IL-12 and IL-18 from *Vα19i* Tg T cells developing in the absence of MR1were significantly lower than from *Vα19i* Tg T cells developing in the presence of MR1.

We observed that tetramer$^+$ CD3$^+$ T cells in *Vα19iCα*$^{-/-}$*MR1*$^{+/+}$ mice expressed more CD44 than tetramer$^+$ CD3$^+$ T cells in *Vα19iCα*$^{-/-}$*MR1*$^{-/-}$ mice in secondary lymphoid organs and liver peripheral tissue (Suppl. Fig. 2A). CD44 expression indicates a memory-like cell phenotype, more likely to readily produce IFN-γ in response to IL-12 and IL-18 and/or Ag-TCR signals. Perhaps surprisingly, *Vα19iCα*$^{-/-}$*MR1*$^{-/-}$ T cells produced more IFN-γ relative to CD4$^+$ and CD8$^+$ αβ T cells from naïve B6-WT mice. However, it has been shown that naïve conventional αβ T cells, unlike previously activated cells, are less responsive to either IL-12 or IL-18 because of low levels of cell surface cognate cytokine receptors (53). Activation of CD4/8 T cells with anti-CD3 and anti-CD28 induces IL-12R expression and responsiveness to IL-12 (53). Tomura and colleagues showed that TCR-triggering and CD28 co-stimulation followed by IL-12 stimulation induces IL-18R expression and responsiveness to IL-18. Although to a significantly lesser extent than *Vα19iCα*$^{-/-}$*MR1*$^{+/+}$ T cells, MR1$^{-/-}$*Vα19i* Tg T cells exhibited a more memory-like phenotype (CD44$^+$) than naïve CD4/8 αβ T cells. Because of this phenotypic difference, higher basal level of IL-12 and/or IL-18 receptors on *Vα19iCα*$^{-/-}$*MR1*$^{-/-}$ T cells may explain their more rapid and higher responsiveness to IL-12 plus IL-18. The relevance of these results is that like other innate T cells, MAIT cells can display immediate function upon infection, and participate in the shaping of the adaptive immune response. The detection of lower level responses in *Vα19iCα*$^{-/-}$*MR1*$^{-/-}$ compared with *Vα19iCα*$^{-/-}$*MR1*$^{+/+}$ T cells confirms that the presence of MR1 is important for optimal development of MAIT cell innate responsiveness to these pro-inflammatory cytokines.

Indeed, tetramer$^+$ MAIT cells in MR1 sufficient mice were found to have a pre-activated phenotype (i.e. >75% expressed CD69 even before *in vitro* stimulation). Moreover, CD44 and CD69 were co-expressed on *Vα19iCα*$^{-/-}$*MR1*$^{+/+}$ tetramer$^+$ CD3$^+$ T cells two-fold more than on *Vα19iCα*$^{-/-}$*MR1*$^{-/-}$ T cells (data not shown). To demonstrate that prior activated MAIT cells developing with MR1 optimally responded to innate cytokines, we performed intracellular IFN-γ staining on sort-purified tetramer$^+$ T cells. CD69$^+$ tetramer$^+$ cells likely represent more recently pre-activated effector memory-like population capable of producing IFN-γ after the addition of IL-12 plus IL-18 (Fig. 3B). We also tested for a panel of cytokines (including IFN-γ) and chemokines in culture supernatant using Multiplex Beads Array kit (EMD Millipore). Tetramer$^+$ T cell subsets from *Vα19iCα*$^{-/-}$*MR1*$^{+/+}$ mice produced higher amounts of IFN-γ than MR1$^{-/-}$ cells after stimulation with IL-12+IL-18 (Suppl. Fig. 2B). Both in *Vα19iCα*$^{-/-}$*MR1*$^{+/+}$ and *Vα19iCα*$^{-/-}$*MR1*$^{-/-}$ mice, tetramer$^+$ DN and CD8$^+$ T cell subsets were the predominant producers of IFN-γ. In addition, MR1$^{+/+}$ tetramer$^+$ DN subsets produced small amounts of GM-CSF, IL-2, IL-4 IL-13 and IL-17, whereas CD8$^+$ subsets produced some GM-CSF, IL-2 and IL-17 (Suppl. Fig. 2B-top panel). Furthermore, MR1 sufficient mice had significantly higher levels of CD69 and higher proportions of CD69$^+$ pre-activated MAIT cells compared with MR1 deficient mice (Fig. 3C and Suppl. Fig. 2C). As illustrated in the middle and bottom panels of Fig. 3C: i) the levels of CD69 are much higher in MR1$^{+/+}$ tetramer$^+$ MAIT cells than in the MR1$^{-/-}$ tetramer$^+$ cells or in the MR1$^{+/+}$ tetramer$^-$(non-RL-reactive) cells and ii) the levels of CD69 in the tetramer$^+$ cells from the MR1$^{-/-}$ are similar to the levels observed in tetramer$^-$ cells from either *Vα19iCα*$^{-/-}$*MR1*$^{+/+}$ or *Vα19iCα*$^{-/-}$*MR1*$^{-/-}$ mice. Therefore, acquisition of this semi-activation status *in vivo* and optimal responsiveness to innate cytokines *in vitro* is

likely dependent upon interaction of TCR with MR1/Ag. In addition, the development of innate cytokine responsiveness in MR1 sufficient mice was greatest in the murine classic MAIT cell populations that were tetramer$^+$ and co-expressed Vβ6/8 and NK1.1 (Fig. 3D). Taken together, these findings demonstrated that MR1 presence is important for development of MAIT cell optimal responses to innate cytokines, presumably because of *in vivo* previous MR1/RL activation. However after *in vivo* activation, responsiveness to innate cytokines is independent of TCR-MR1 engagement.

Vα19i Tg cells that develop in MR1$^{+/+}$ mice functionally respond to MR1-restricted RL Ag more robustly than those developing in MR1$^{-/-}$ mice

To address the question whether tetramer$^+$ cells from MR1 sufficient and deficient mice are functionally responsive to vitamin B2 metabolites, FACS sorted tetramer$^+$ T cell subsets from the blood of *Vα19iCα*$^{-/-}$*MR1*$^{+/+}$ and *Vα19iCα*$^{-/-}$*MR1*$^{-/-}$ mice were tested for their response to the potent rRL-6HM Ag (2). The sorted tetramer$^+$ cells were rested in medium overnight before addition of CH27-mMR1 cells as APC. This CH27 cell line over-expressing murine MR1 was shown in previous work (2, 18, 20) to optimize stimulation of MAIT cells *in vitro*. The vitamin B2 metabolite rRL-6HM with or without anti-MR1 antibodies was added for 60h. A panel of cytokines and other effector molecules secreted into the supernatants of these cultures were studied using a multiplex cytokine assay.

Tetramer$^+$ T cells from *Vα19iCα*$^{-/-}$*MR1*$^{+/+}$ mice responded to rRL-6HM Ag much more robustly than tetramer$^+$ T cells from *Vα19iCα*$^{-/-}$*MR1*$^{-/-}$ mice by secreting much higher levels of cytokines, chemokines and cytolytic effector molecules (Fig. 4A). These rRL-6HM-specific responses were completely blocked with mAb to MR1; confirming MR1 presentation of the active vitamin B2 metabolite to MAIT cells. As shown in Fig. 4B, stimulation of purified splenic MR1$^{+/+}$ *Vα19i* Tg T cells by rRL-6HM Ag presented by CH27-mMR1 was blocked with anti-MR1 antibody, but not mouse IgG isotype control, confirming the requirement for MR1 presentation. Interestingly, the soluble effectors produced by different co-receptor subsets of tetramer$^+$ T cells that developed in the presence of MR1 were markedly diverse, further indicating that tetramer$^+$ MAIT cells include functionally heterogeneous subsets. The CD4$^+$ subset predominantly produced IL-4 followed by IL-2, while both DN and CD8$^+$ subsets produced IFN-γ, MIP-1α/CCL3, MIP-1β/CCL4, and increased levels of granzyme B (GZMB), but not IL-2 (Fig. 4A, upper panel). The MR1$^{+/+}$ DN subset also produced increased amounts of IL-4 and in addition a small amount of IL-13 cytokine. Thus, tetramer$^+$ CD4$^+$ MAIT cells produced cytokines characteristic of Th1/Th2 responses, the DN subset produced a pattern of Th1/Th2/Tc1 T cell responses while the tetramer$^+$ CD8$^+$ subset produced a Tc1-like cytokine profile. Mature thymocytes from both MR1$^{+/+}$ and MR1$^{-/-}$ *Vα19i* Tg mice did not produce appreciable amounts of IFN-γ in response to *M. bovis* BCG-infected APC (data not shown). These latter results confirm that thymic *Vα19i*$^+$ MAIT cells have an unbiased phenotype characteristic of naïve unactivated T cells. These experimental findings demonstrate that peripheral tetramer$^+$ *Vα19i* Tg cells developing in MR1 sufficient mice are functionally capable MAIT cells that like human MAIT cells respond to RL compounds in an MR1-restricted manner (2). On the contrary, tetramer$^+$ *Vα19i* Tg cells from MR1 deficient mice displayed markedly reduced effector functions after MR1/RL *in vitro* activation (Fig. 4A,

bottom panel). These combined results suggest that MR1 is necessary for the development of MAIT cell effector functions. However, another possibility suggested by the fact that MR1/RL tetramer$^+$ MAIT cells do develop in the absence of MR1, albeit in significantly lower frequencies, is that peripheral activation by MR1/RL is necessary *in vivo* for the development of MAIT cell effector functions and peripheral expansion. Furthermore, to our knowledge, this is the first report that MIP-1α/CCL3, MIP-1β/CCL4 and GZMB are produced by mouse MAIT cells. Perhaps more importantly, the differences in effector functions observed in different MAIT cell co-receptor subsets predict that these subsets also may provide functional differences in controlling microbial infections.

The Vβ6/8$^+$, NK1.1$^+$ subpopulation of Vα19i Tg MAIT cells is highly enriched in peripheral sites

Among tetramer$^+$ CD3$^+$ mature thymocytes, mLN, splenic and blood cells from uninfected *Vα19iCα*$^{-/-}$*MR1*$^{+/+}$ mice, we found that less than half expressed Vβ6/8 (Fig. 1E, Suppl. Fig. 1B-middle dot plots column, and 1C-middle panel). Also, less than 25% expressed NK1.1 in the thymus, mLN and spleen (Fig. 1E, Suppl. Fig. 1B-right dot plots column and 1C-bottom panel). Furthermore, shown in Suppl. Fig. 3A–3C and Fig. 5A, less than 20% of all 3 co-receptor subsets of tetramer$^+$ MAIT cells in thymus and secondary lymphoid organs harvested from *Vα19i* Tg MR1 sufficient mice expressed both Vβ6/8 and NK1.1. In contrast, in blood from these same mice, approximately half of all tetramer$^+$ MAIT cells expressed both Vβ6/8 and NK1.1, and more than 80% of tetramer$^+$, Vβ6/8$^+$ MAIT cells co-expressed NK1.1 (Fig. 5A and 5B). An even higher percentage of tetramer$^+$ CD3$^+$ MAIT cell subsets co-expressing Vβ6/8 and NK1.1 was observed in liver peripheral tissue (Suppl. Fig. 3A–3C, 3E). Additionally, > 84% of tetramer$^+$ Vβ6/8, NK1.1 double possible cells expressed both CD44 and CD69 in peripheral blood and the liver (data not shown). On the other hand, less than 11% of tetramer$^+$ Vβ6/8, NK1.1 double negative cells expressed both CD44 and CD69. These results suggest that the tetramer$^+$, Vβ6/8$^+$, NK1.1$^+$ cells are the subset of MAIT cells most highly reactive with MR1, and as a consequence optimally expand and express a more activated phenotype in the peripheral sites. In support of this notion, despite significantly lower levels of CD3 expression, the Vβ6/8, NK1.1 double positive subset of tetramer$^+$ cells that developed in the presence of MR1 was shown to have significantly higher levels of MR1/RL tetramer staining than the Vβ6/8, NK1.1 double negative subset both in the spleen and liver (Fig. 5C and Suppl. Fig. 3D). The combination of lower CD3 and higher tetramer staining indicate that the Vβ6/8, NK1.1 double positive subsets of tetramer$^+$ cells express TCRs with higher affinity. These combined results further indicate that the Vβ6/8 and NK1.1 double positive subset of tetramer$^+$ cells constitute the most highly functional MAIT cell subset *in vivo*. We speculate that this circulating Vβ6/8, NK1.1 double positive MAIT cell population may be a further differentiated effector subset because of previous MR1/RL activation, consistent with better responsiveness to IL-12+IL-18 cytokines (Fig. 3D). As shown in Suppl. Fig. 3E, NK1.1 was minimally expressed on mature Vβ6/8$^+$ tetramer$^+$ MAIT cells in the thymus, but progressively increased with peripheral activation in both MR1 sufficient and deficient Tg mice, most strikingly in MR1 sufficient mice. In the absence of MR1, there was a 76% and 84% relative reduction in the proportion of peripherally expanded/activated Vβ6/8 NK1.1 double positive tetramer$^+$ CD3$^+$ T cells in blood and the liver, respectively. Taken together, our data indicate

that peripheral MR1 is necessary for optimal expansion/activation of MAIT cells, and NK1.1 is likely to represent an activation rather than developmental MAIT cell marker.

Vα19i Tg MAIT cells developing in MR1 sufficient mice are optimally recruited to mycobacteria-infected lungs and provide maximal early protection

We have previously shown that purified *Vα19i* Tg MAIT cells developing with MR1 inhibit intracellular growth of mycobacteria *in vitro*, whereas control *Vα19i* Tg T cells from MR1$^{-/-}$ mice showed no inhibition of bacterial growth in *M. bovis* BCG-infected macrophages (24). This observation indicated that the maximal antibacterial function of Vα19-Jα33 TCR-bearing T cells requires MR1 selection during development. T cells from naïve (unvaccinated and uninfected) B6-MR1$^{-/-}$ and B6-WT mice also failed to inhibit the intracellular growth of *M. bovis* BCG in macrophages. We also demonstrated *in vivo* that, on day 10 following aerosol infection with *M. bovis* BCG, B6 mice deficient in MR1 had higher mycobacterial burden in the lungs than wild type mice, indicating that MR1-restricted MAIT cells are important for optimal protection against mycobacterial infection (24).

Of note, previous studies of both mouse and human MAIT cells have shown that MAIT cells increase at the site of infections (19, 20, 35, 37). In the present study, we used MR1/RL tetramers to identify Ag-specific MAIT cell subsets at the site of mycobacterial infection in the lung. Groups of B6-MR1$^{-/-}$, B6-WT, *Vα19iCα*$^{-/-}$*MR1*$^{-/-}$ and *Vα19iCα*$^{-/-}$*MR1*$^{+/+}$ mice were infected intranasally with *M. bovis* BCG Danish. MR1/RL-specific MAIT cells were increased in the infected lung airways at 10 days post-infection, a time point when MAIT cells were previously shown to be important for control of the infection (24). Moreover, the early accumulation in mouse lungs of a variety of different innate cells including MAIT cells after mycobacterial infection appears to occur between day 10 and 15 (54). Mycobacterial burden in the lung at day 10 post infection was significantly lower in *Vα19i* Tg MR1 sufficient mice than in the lungs of the infected *Vα19i* Tg mice lacking MR1, suggesting MR1 dependent *in vivo* function of *Vα19i* Tg T cells (Fig. 6Ai). Confirming our previous results, mycobacterial burden in the lungs of B6-WT mice was significantly lower than in B6-MR1$^{-/-}$ mice. Interestingly, both *Vα19iCα*$^{-/-}$*MR1*$^{-/-}$ and B6-WT mice had similar mycobacterial loads, which were lower than found in B6-MR1$^{-/-}$ mice. We were surprised that *Vα19i* Tg T cells developing in the absence of MR1 conferred protection against mycobacterial infection comparable to the non-Tg MAIT cells in B6-WT mice. As shown in Fig. 6D, it is likely that the slightly increased number of tetramer^{+} *Vα19i* Tg T cells developing in the absence of MR1 could provide partial protection *in vivo*. In addition, we found that tetramer^{+} MAIT cells developing in the absence of MR1 can respond to RL Ag in an MR1 dependent manner (Fig. 4A-bottom panel right) and respond in an MHC class Ia dependent manner (Suppl. Fig. 4-i). Indeed, inhibitory effects of purified total T cells from *Vα19iCα*$^{-/-}$*MR1*$^{-/-}$ mice were completely abrogated in macrophages deficient in MR1 or classical MHC class Ia molecules (Suppl. Fig. 4A-ii). These combined results demonstrate that the tetramer^{+} *Vα19i* T cells generated in MR1 knockout mice can develop effector functions *in vivo* in response to infection despite the absence of MR1. Most importantly, after aerosol lung infection with virulent *M. tuberculosis* Erdman strain, lung mycobacterial load was significantly lower in *Vα19iCα*$^{-/-}$*MR1*$^{+/+}$ mice than in B6-WT

control mice (Fig. 6A-ii). These differences strongly corroborate a role for MAIT cells in controlling pulmonary mycobacterial infections.

MR1/RL tetramers were used to enumerate MAIT cells in the BAL fluid of uninfected vs. infected mice. Representative plots of $CD3^+$ lymphocytes and $tetramer^+$ $CD3^+$ T cells in BAL fluids from uninfected or BCG-infected mice are shown in Suppl. Fig. 4B. BAL fluid from all uninfected mouse groups had very low numbers of detectable T cells (Fig. 6B). Although the total number of BAL mononuclear cells increased in the lungs of all four infected groups of mice compared with uninfected controls (Fig. 6C), the highest numbers of all $CD3^+$ T cell subsets (DN > $CD4^+$/$CD8^+$) were detected in the infected *Vα19iCα*$^{-/-}$*MR1*$^{+/+}$ mice (Fig. 6B). Consistent with their expected low frequency of MAIT cells, very few $tetramer^+$ cells were detected in the BAL fluid of uninfected or infected B6-WT or B6-MR1$^{-/-}$ mice (Fig. 6D). However, remarkably higher numbers of $tetramer^+$ T cells were detected in BAL fluid from infected *Vα19iCα*$^{-/-}$*MR1*$^{+/+}$ mice than all other groups of mice (Fig. 6D). DN $tetramer^+$ cells were the predominant subset (43%) followed by $CD8^+$ (33%) and then $CD4^+$ subset (24%) (Fig. 6E; top pie chart). This hierarchy of $tetramer^+$ co-receptor subset distribution was similar to what was found in the blood of infected mice (data not shown). Importantly, more MAIT cells were identified in *Vα19i* Tg mice lacking MR1 than in B6-WT and B6-MR1$^{-/-}$ mice, and these increased numbers of MAIT cells were associated with better mycobacterial control (Fig. 6Ai). $Tetramer^+$ BAL T cells detected in *Vα19iCα*$^{-/-}$*MR1*$^{-/-}$ mice were $CD8^+$ (38%) with comparable fractions of $CD4^+$ (31%) and DN (31%) subsets (Fig. 6E; bottom pie chart). Furthermore, B6-WT mice had more $tetramer^+$ MAIT cells (~0.25 x 10^4 $tetramer^+$ $CD3^+$ cells) than B6-MR1$^{-/-}$ mice, which explains better protection in wild type B6 mice than in non-transgenic MR1 knockout mice, confirming our previous report (24). We conclude that MAIT cells are recruited early into the lung after mycobacterial challenge and provide important protective effects. In addition, MAIT cells developing in the presence of MR1 are optimally protective.

Phenotype of $tetramer^+$ MAIT cell subsets in lung airways associated with optimal protection against primary mycobacterial challenge

Vβ6/8$^+$, NK1.1$^+$ and Vβ6/8$^-$, NK1.1$^-$ subpopulations of T cells each represented ~50% of the $tetramer^+$ MAIT cells accumulating in the airways of *Vα19i* Tg MR1 sufficient mice (Fig. 7A). Only minor populations of $tetramer^+$ cells were NK1.1$^+$, Vβ6/8$^-$or NK1.1$^-$, Vβ6/8$^+$ (<6%) in the infected lung. This was true for all CD4, CD8 and DN co-receptor subsets of $tetramer^+$ T cells. Which of these NK1.1$^+$, Vβ6/8$^+$ versus Vβ6/8$^-$, NK1.1$^-$ subsets are most important for protection against mycobacterial infection requires further investigation. Gating on NK1.1$^+$, Vβ6/8$^+$ and Vβ6/8$^-$, NK1.1$^-$ subsets, we found that the majority of the $tetramer^+$ *Vα19i* Tg cells in the BAL fluid of infected MR1 sufficient mice also expressed both α4β1 integrin and the chemokine receptor CXCR3 (Fig. 7B), molecules previously associated with trafficking activated Ag-specific T cells to infected lungs. Integrin α4β1 is required for cells to cross from blood to lung airway where its ligand VCAM-1 is up-regulated upon infection (55); and CXCR3 mediates recruitment of effector T cells into inflammatory tissues in response to its ligands induced by infection (56), and is known to be co-expressed with α4β1 in blood and BAL samples after mycobacterial infection. Thus these combined data demonstrate that DN > $CD8^+$ > $CD4^+$, Vβ6/8, NK1.1

double positive and double negative tetramer$^+$ cells were associated with lung protection in *Vα19iCα*$^{-/-}$*MR1*$^{+/+}$ mice. Moreover, most MAIT cells recruited and/or expanded in the infected lung express both α4β1 integrin and chemokine receptor CXCR3. Interestingly, in the BAL fluids from infected wild type B6 mice, almost all MAIT cell subsets (DN > CD4$^+$ > CD8$^+$) were Vβ6/8$^+$, NK1.1$^+$ double positive and expressed both α4β1 integrin and CXCR3 (Fig. 7D, 7E and 7F). These latter results are consistent with a previous study reporting that in response to *Francisella tularensis* lung infection, CD4/8 DN, Vβ6/8$^+$ MAIT cells were associated with optimal early control of bacterial infection in unvaccinated mice (37). Because of limited cell numbers available in BAL, and the fact that MR1/RL tetramer staining does not survive fixation/permeabilization treatment, we have not been able to identify cytokine or in situ proliferation profiles after mycobacterial infection.

Comparisons of Blood and BAL tetramer$^+$ T cell subsets in uninfected and infected Vα19iCα$^{-/-}$ MR1$^{+/+}$ mice

We further characterized the phenotypes and numbers of CD3$^+$, tetramer$^+$ T cell subsets in the blood and BAL of uninfected vs. infected *Vα19iCα*$^{-/-}$*MR1*$^{+/+}$ mice. The relative distributions of CD4/8 co-receptor subsets of Vβ6/8 positive and negative, tetramer$^+$ cells in the blood of uninfected and infected mice was DN > CD8$^+$ > CD4$^+$ (data not shown), similar to infected BAL populations. In addition, comparable percentages of tetramer$^+$, Vβ6/8 and NK1.1 double positive and double negative subsets were present in uninfected and infected blood (Fig. 8A). However, the frequencies of most of the tetramer$^+$ subsets in blood were reduced by 50% or more in infected compared with uninfected mice (Fig. 8B). Thus, our data indicate that comparable numbers of tetramer$^+$, Vβ6/8/NK1.1 double positive and double negative populations appear to exit the blood after infection, and both subsets accumulate in the infected lungs of *Vα19iCα*$^{-/-}$*MR1*$^{+/+}$ mice, as shown in Fig. 8C and 8D. In wild type B6 mice, only the Vβ6/8$^+$, NK1.1$^+$ population of tetramer$^+$ MAIT cells were detected at the site of infection (Fig. 7E). In summary, our tetramer studies of wild type B6 mice further confirm the biological significance of our transgenic mouse studies. Our combined findings allow us to propose a model that MAIT cells developing in the presence of MR1 are optimally protective, the population relevant for protection is heterogeneous and that MAIT cell subsets controlling murine mycobacterial pulmonary infection traffic from blood to the lungs.

Discussion

Our novel MR1/RL Ag tetramer characterization of the *Vα19i* Tg mouse model, offers new insights in the development and function of MAIT cells, and their role in TB protective immunity. We demonstrate that mouse MAIT cells contain heterogeneous populations distinguished by their expression of diverse Vβ TCR, NK1.1 or not, and CD4/8 co-receptors. In addition, we show that there are more MR1/RL tetramer$^+$ MAIT cells in *Vα19i* Tg mice expressing MR1 than in those lacking MR1. The relative distributions of MAIT cell subsets are similar between thymus, mLN, spleen, blood, liver and mycobacterial infected lung airways, although the relative numbers in blood versus lung airways decrease post-infection. CD44 and CD69 expression on MAIT cells was higher in liver peripheral tissue than on MAIT cells in the thymus and naïve secondary lymphoid organs in MR1 expressing mice.

This likely represents a progressive activation of peripheral MAIT cells. The patterns of soluble effector molecules released by peripheral blood tetramer$^+$ MAIT cell subsets after stimulation with rRL-6HM Ag were characteristic of Th1 (IL-2, IFN-γ) Th2 (IL-4) and Tc1 (IFN-γ, GZMB) immune responses. In contrast to the total *Vα19i* Tg T cells used by the Gilfillan lab to determine cytokine production profiles (25), our sort-purified blood tetramer$^+$ Tg T cell subsets did not produce IL-5 and IL-10 in response to rRL-6HM Ag. Also, contrary to our earlier work in which we stimulated purified total *Vα19iCα*$^{-/-}$*MR1*$^{+/+}$ T cells with *M. bovis* BCG-infected BMDMφ (24), these circulating tetramer$^+$ MAIT cells did not produce IL-17A after rRL-6HM Ag stimulation *in vitro*. A similar observation was recently reported for human MAIT cell clones stimulated with riboflavin-producing *Escherichia coli*-infected APC (47). Lucia Mori and colleagues speculated that the failure to produce IL-17A by MAIT cells following Ag/TCR stimulation may reflect requirement for additional environmental signals such as IL-7 signalling (57). The results reported here impact on several outstanding issues discussed below.

Is MR1 required for the thymic selection of MAIT cells or only for their peripheral expansion?

Similar to type I NKT cells, MAIT cells were recently demonstrated to be positively selected by CD4$^+$ CD8$^+$ thymocytes (58). However, distinct from CD1d, MR1 is very poorly expressed at the cell surface even on double positive thymocytes. Furthermore, the thymic Ag presented by MR1, which was speculated to be of endogenous origin, remains unknown. In addition, the number of MAIT cells in the thymus of both humans and mice is very low (8, 13, 59). Thus conditions for thymic selection of MR1-restricted MAIT cells may not be optimal. By contrast, Ag presentation in the periphery is clearly important for MAIT cell expansion and function. MAIT cells in the periphery remain naïve until exposed to the commensal flora resulting in their dramatic expansion and conversion to an effector/memory phenotype (13, 60). Thus, the role of MR1 in thymic selection may be of lesser importance than its role in peripheral expansion. Relevant to this hypothesis, we found that tetramers stained a significant proportion of mature T cells in the thymus from *Vα19iCα*$^{-/-}$*MR1*$^{-/-}$ mice, indicating that MR1 is not absolutely required for MAIT cell thymic selection (Fig. 2C, D and Suppl. Fig. 1B, C). This finding is similar to a previous report that type I NKT cells develop in *Vα14i* Tg mice in the absence of CD1d (61). Since the TCR Vα chain of type I NKT cells is predominant in CD1d/lipid recognition (62), the overexpression of *Vα14i* transgene was considered to be sufficient to bypass the requirement for type I NKT selection on CD1d in Tg mice. Since TCR Vα19i is also predominant in MAIT cell detection of MR1/RL (6), a similar mechanism might explain our findings of tetramer$^+$ cells in *Vα19iCα*$^{-/-}$*MR1*$^{-/-}$ mice. Alternatively, given that the α1 and α2 domains of MR1 share high similarity in both sequence and structure with classical MHC-I molecules and that the footprint of MAIT TCR on MR1 closely resembles the typical TCRs on classical MHC-I (3, 42, 63, 64), we speculate that in the absence of MR1, tetramer$^+$ T cells can be selected by a weak cross-reaction on MHC-Ia. Whether this type of selection occurs in non-transgenic mice or is physiological relevant remains to be demonstrated.

Is Vβ6/8 pairing required for MAIT cell generation?

Previous investigations have suggested that most MAIT cells expressed Vα19i paired with Vβ6/8. However, we found that large proportions of tetramer$^+$ MAIT cells among both mature thymocytes and peripheral T cells did not express Vβ6/8. Furthermore, only half of the tetramer$^+$ MAIT cells recruited to the lungs after mycobacterial infection in *Vα19iCα*$^{-/-}$*MR1*$^{+/+}$ mice co-expressed Vβ6/8. MR1/RL tetramers stained not only Vβ6/8$^+$ T cells but a significant number of other Vβ chains in *Vα19i* Tg mice. Furthermore, we previously demonstrated that tetramer$^+$, Vβ6/8$^-$ MAIT cells in *Vα19i* Tg MR1 sufficient mice produced IFN-γ and TNF-α after rRL-6HM Ag stimulation in an MR1-restricted fashion (Fig. 8 in ref. (4)). These results suggest that functionally important MAIT cells are more heterogeneous in terms of Vβ expression than previously thought. On the other hand, here we demonstrate that Vβ6/8$^+$ MAIT cells that developed in the presence of MR1 bound MR1/RL tetramers with higher affinity (Fig. 5C and Suppl. Fig. 3D) and exhibited higher levels of CD69 expression indicative of a previously activated state (Fig. 3B and 3C). In addition, in our work cited above, Vβ6/8$^+$ tetramer$^+$ MAIT cells secreted higher levels of inflammatory cytokines in response to rRL-6HM restricted by MR1 (4). Moreover, we also show here that Vβ6/8$^+$, NK1.1$^+$, tetramer$^+$ MAIT cells responded to IL-12 plus IL-18 better than the Vβ6/8$^-$, NK1.1$^-$ population (Fig. 3D). Furthermore, in WT B6 mice that were significantly better protected than non-transgenic MR1 knockout mice, only Vβ6/8$^+$ MAIT cells were recruited into the lungs after mycobacteria challenge. Therefore, further studies are needed to determine whether tetramer$^+$, Vβ6/8$^-$ MAIT cells can provide functionally important, MR1-restricted protective responses against mycobacterial and other infectious pathogens.

Mouse NK1.1 may be an important phenotypic marker associated with peripheral expansion of Vβ6/8-expressing functional MAIT cells

Defining MAIT cells by their preferential Vβ6/8 expression (classical MAIT cells) in *Vα19i* Tg mice, a good proportion of MAIT cells from the spleen and mesenteric lymph nodes were previously shown to express NK1.1 (25, 65). However, NK1.1 was not considered to be a reliable phenotypic marker for MAIT cells since only a subset of Vβ6/8$^+$ cells were found to express NK1.1 in *Vα19i* Tg MR1 sufficient mice (13, 25). Indeed, in the present study, only about 3% and less than 20% of the CD3$^+$ tetramer$^+$ cells from the thymus and secondary lymphoid tissues of *Vα19iCα*$^{-/-}$*MR1*$^{+/+}$ mice were NK1.1$^+$, respectively (Supp. Fig. 1C-bottom panel). Nevertheless, NK1.1 expression was substantially increased on the tetramer$^+$, Vβ6/8$^+$ fraction compared with the Vβ6/8$^-$ population, especially in the most peripheral sites (Fig. 5A, B and Suppl. Fig. 3B, C, E). These peripheral Vβ6/8$^+$, NK1.1$^+$, tetramer$^+$ cells represent effector memory cells, based on their higher co-expression of CD44 and CD69 and better functional response to *in vitro* rRL-6HM or cytokine stimulation. We propose that this segregation of MAIT cell phenotypes is driven by MR1-restricted presentation of bacterial flora RL antigens. In support of this model we show that bulk Vβ6/8$^+$, NK1.1$^+$ Tg T cells bind MR1/RL tetramers with higher affinity than Vβ6/8$^-$, NK1.1$^-$ Tg T cells (Fig. 5C and Suppl. Fig. 3D). These findings support the model that presumed exposure to commensal flora-derived RL antigens promotes the peripheral expansion of Vβ6/8$^+$, NK1.1$^+$ cells driven by increased affinity for MR1/RL complexes.

However, in light of recent findings that human MAIT cells develop and mature in the fetus, prior to exposure to the commensal flora (59), the presence of commensal flora may not be absolutely necessary for acquisition of innate-like microbial reactivity or expansion/maturation of MAIT cells. On the other hand, it is worth noting that the Sandberg lab did not rule out the possibility of fetal mucosal exposure to components of the maternal microbial vitamin B2 metabolites delivered via the amniotic fluid. They further concluded that association between maturation and gain of effector functions argues for the involvement of an MR1-presented ligand. They also found that there was a progressive increase in the proportion of MAIT cells detected in the fetal thymus, spleen and peripheral sites including small intestine, liver and lung.

Is NK1.1 expression on mouse MAIT cells a developmental lineage and/or activation marker?

Mouse NK1.1 (also known as KLRB1C and NKR-P1C) is expressed on NK and NKT cells in C57BL/6 mice. Although crosslinking of the receptor using an NK1.1-specific mAb induces NK cell-mediated cytotoxicity and effector cytokine secretion, the *in vivo* function of NK1.1 and the nature of its ligand(s) remain unknown (66–70). Thus whether NK1.1 is a developmental lineage marker and/or an activation receptor is an important question. Of note, in the present study, we found that NK1.1 was marginally expressed on tetramer^{+} thymocytes, but was gradually enriched with progressive peripheral activation in *Vα19iCα*$^{-/-}$*MR1*$^{+/+}$ mice. Increase in the proportional expression of NK1.1 from the most naïve (thymus) to the most peripherally expanded/activated MAIT cell populations (Fig. 5A, 5B, Suppl. Fig. 3B, C, E and 7A), suggests an up-regulation of NK1.1 expression upon progressive exposure to antigens. Thus NK1.1 likely represent activation rather than developmental MAIT cell markers. Our findings reported here further suggest that NK1.1 is a reliable marker for MR1-dependent classical MAIT cells with optimal innate-like cell function. However, both Vβ6/8, NK1.1 double positive and double negative, tetramer^{+} MAIT cells were recruited into the lungs of *Vα19i* Tg MR1 sufficient mice that were found to be optimally protected against mycobacterial challenges (see below). We conclude that mouse NK1.1 may be an important phenotypic marker associated with peripheral expansion/activation of classical Vβ6/8-expressing functional MAIT cells, rather than a MAIT cell lineage marker.

MR1-restricted MAIT cells have important anti-mycobacterial effects

MAIT cells are known to accumulate at the site of infection (19, 20). Because in some of these same studies an accompanying decrease in MAIT cell number was also seen in the blood of infected individuals, MAIT cell migration was implicated. Consistent with these studies we show here that all tetramer^{+} subsets (DN/CD8^{+}/CD4^{+} and both Vβ6/8^{+} and Vβ6/8^{-}) were appreciably decreased in blood after BCG infection (Fig. 8B). We also noted that the majority of all MAIT cell blood subsets expressed both α4β1 integrin and the chemokine receptor CXCR3 (data not shown). The expression of α4β1 integrin is known to localize Ag-specific T cells to the airway where its ligand VCAM-1 is up-regulated upon infection (55, 71, 72). CXCR3 is a dominant chemokine receptor strongly expressed on activated Th1 cells, thus directing them towards the lung in mycobacterial and other respiratory infections (54, 73–75). CXCR3-expressing lymphocytes migrate towards three

chemokines namely, CXCL9/monokine induced by IFN-γ (Mig), CXCL10/IFN-γ-inducible protein 10 (IP-10), and CXCL11/IFN-γ-inducible T cell α-chemoattractant (I-TAC) (76–78). In the lung, CXCR3 ligands are known to be produced by bronchial epithelial cells following infection or vaccination in response to IFN-γ (54, 79, 80). Thus the expression of α4β1 and CXCR3 on all MAIT subsets could explain why all MAIT subsets are diminished in the blood after pulmonary mycobacterial infection.

In *Vα19iCα*$^{-/-}$*MR1*$^{+/+}$ mice after pulmonary mycobacterial challenge, the disappearance of all subsets of MAIT cells from blood was associated with their accumulation among infected BAL cells and early protection against mycobacterial infection (Fig. 6, 7A, 8C and 8D). Interestingly, MAIT cell subsets expressing only Vβ6/8 TCR and NK1.1 accumulated in the airways of infected B6-WT mice (Fig. 7E). This is consistent with a recent report by Cowley's group that only Vβ6/8^{+} and not Vβ6/8^{-} MAIT cells were detected in lung homogenates of wild type B6 mice after *F. tularensis* infection (37). However, only 12.6% of these MAIT cells recruited in response to *F. tularensis* infection expressed NK1.1. Nevertheless, the concordance of their findings with *F. tularensis* infection of wild type mice is strikingly similar to our findings with BCG infection of wild type mice, strongly supporting the unique ability of Vβ6/8^{+} and not Vβ6/8^{-} to accumulate at the site of infection. Our studies further demonstrate that all MAIT cell subsets leave the blood after mycobacteria infection of the lung, presumably based on their expression of α4β1 and CXCR3. While there are differences between Tg and wild type mice, our findings demonstrate that the tetramer^{+} DN MAIT cell subset was the predominant population in the lungs of both MR1 expressing *Vα19i* Tg and non-transgenic B6 mice after mycobacterial pulmonary infection. These combined results suggest that the tetramer^{+} DN MAIT cell subset is the most important for TB immunity. This possibility will be confirmed in future studies comparing protective effects of adoptively transferred, sort-purified MAIT cell subsets. However, both Vβ6/8^{+}NK1.1^{+} and Vβ6/8^{-}NK1.1^{-} subsets were detected in the lung airways of Tg mice while only the Vβ6/8^{+}NK1.1^{+} subpopulation accumulated at the site of infection in wild type B6 mice after mycobacterial infection and are associated with early protection. We will in the future use adoptive transfer studies to characterize which of these tetramer^{+} CD3^{+} Vβ6/8^{+}NK1.1^{+} and Vβ6/8^{-}NK1.1^{-} MAIT cell subpopulations is more important in protective anti-mycobacterial immunity. Moreover, we will perform TCRβ analysis to determine the CDR3β repertoire after vaccination/challenge to gain better understanding of the biology of mycobacteria-specific MAIT cells.

In conclusion, our study provides insight into the mechanisms of how MAIT cells activated by innate cytokines and/or MR1/RL-TCR signals function to control mycobacterial infection *in vivo*. MAIT cells recruited to the lung airways have the potential to produce IL-2, IFN-γ, MIP-1α/CCL3 and MIP-1β/CCL4 chemokines (signal through CCR1 and CCR5 chemokine receptors) and GZMB. These MAIT cell-derived soluble mediators could facilitate the early production of NO, and the timely recruitment of CCR1^{+} and CCR5^{+} macrophages, immature dendritic cells, granulocytes, Ag-specific CD8^{+} and Th1 CD4^{+} T cells to the lungs during mycobacteria infection. This study also revealed a previously unrecognized potential role for MAIT cells in the killing of mycobacteria-infected cells in the lung via the cytotoxic granule exocytosis effector pathway. The observation by Olivier Lantz's laboratory that

MAIT cells are cytotoxic *in vitro* (60), is fitting with our novel findings that these cells produce large amounts of the granule serine protease, GZMB. Thus, we infer that MAIT cell-mediated control of mycobacterial infection *in vivo* mechanistically involves the NOS2/NO and granule serine protease exocytosis effector pathways. Furthermore, MAIT cells can facilitate the recruitment of $CCR1^+$ and $CCR5^+$ immune cells to the lung during mycobacterial infection. Our study provides evidence that future TB therapeutic/prophylactic vaccine efforts could target the induction of MAIT cell responses. Such vaccines may require incorporation of vitamin B2 metabolites as MAIT cell immunogens and/or IL-12 plus IL18 expressing plasmid combinations to augment immune response. The use of cytokine-expressing plasmids as a strategy to augment T cell responses has been demonstrated in HIV vaccine research (81–83).

Supplementary Material

Refer to Web version on PubMed Central for supplementary material.

Acknowledgments

We thank Drs Susan Gilfillan and Wayne Yokoyama (Washington University School of Medicine) for the generous gift of *Vα19i* Tg and H2-$K^{b-/-}$ H2-$D^{b-/-}$ mouse strains, respectively. We thank Dr. Liping Yang (Yokoyama lab, Washington University School of Medicine) for assistance with isolation of lymphocytes by perfusion and Dr Dale I. Godfrey (University of Melbourne) for critical advice.

References

1. Hashimoto K, Hirai M, Kurosawa Y. A gene outside the human MHC related to classical HLA class I genes. Science. 1995; 269:693–695. [PubMed: 7624800]
2. Kjer-Nielsen L, Patel O, Corbett AJ, Le Nours J, Meehan B, Liu L, Bhati M, Chen Z, Kostenko L, Reantragoon R, Williamson NA, Purcell AW, Dudek NL, McConville MJ, O'Hair RA, Khairallah GN, Godfrey DI, Fairlie DP, Rossjohn J, McCluskey J. MR1 presents microbial vitamin B metabolites to MAIT cells. Nature. 2012; 491:717–723. [PubMed: 23051753]
3. Patel O, Kjer-Nielsen L, Le Nours J, Eckle SB, Birkinshaw R, Beddoe T, Corbett AJ, Liu L, Miles JJ, Meehan B, Reantragoon R, Sandoval-Romero ML, Sullivan LC, Brooks AG, Chen Z, Fairlie DP, McCluskey J, Rossjohn J. Recognition of vitamin B metabolites by mucosal-associated invariant T cells. Nature communications. 2013; 4:2142.
4. Reantragoon R, Corbett AJ, Sakala IG, Gherardin NA, Furness JB, Chen Z, Eckle SB, Uldrich AP, Birkinshaw RW, Patel O, Kostenko L, Meehan B, Kedzierska K, Liu L, Fairlie DP, Hansen TH, Godfrey DI, Rossjohn J, McCluskey J, Kjer-Nielsen L. Antigen-loaded MR1 tetramers define T cell receptor heterogeneity in mucosal-associated invariant T cells. The Journal of experimental medicine. 2013; 210:2305–2320. [PubMed: 24101382]
5. Birkinshaw RW, Kjer-Nielsen L, Eckle SB, McCluskey J, Rossjohn J. MAITs, MR1 and vitamin B metabolites. Current opinion in immunology. 2014; 26:7–13. [PubMed: 24556396]
6. Corbett AJ, Eckle SB, Birkinshaw RW, Liu L, Patel O, Mahony J, Chen Z, Reantragoon R, Meehan B, Cao H, Williamson NA, Strugnell RA, Van Sinderen D, Mak JY, Fairlie DP, Kjer-Nielsen L, Rossjohn J, McCluskey J. T-cell activation by transitory neo-antigens derived from distinct microbial pathways. Nature. 2014; 509:361–365. [PubMed: 24695216]
7. McWilliam HE, Birkinshaw RW, Villadangos JA, McCluskey J, Rossjohn J. MR1 presentation of vitamin B-based metabolite ligands. Current opinion in immunology. 2015; 34C:28–34. [PubMed: 25603223]
8. Tilloy F, Treiner E, Park SH, Garcia C, Lemonnier F, de la Salle H, Bendelac A, Bonneville M, Lantz O. An invariant T cell receptor alpha chain defines a novel TAP-independent major

histocompatibility complex class Ib-restricted alpha/beta T cell subpopulation in mammals. The Journal of experimental medicine. 1999; 189:1907–1921. [PubMed: 10377186]

9. Rossjohn J, Gras S, Miles JJ, Turner SJ, Godfrey DI, McCluskey J. T Cell Antigen Receptor Recognition of Antigen-Presenting Molecules. Annual review of immunology. 2014
10. Gold MC, Lewinsohn DM. Co-dependents: MR1-restricted MAIT cells and their antimicrobial function. Nature reviews. Microbiology. 2013; 11:14–19.
11. Reantragoon R, Kjer-Nielsen L, Patel O, Chen Z, Illing PT, Bhati M, Kostenko L, Bharadwaj M, Meehan B, Hansen TH, Godfrey DI, Rossjohn J, McCluskey J. Structural insight into MR1-mediated recognition of the mucosal associated invariant T cell receptor. The Journal of experimental medicine. 2012; 209:761–774. [PubMed: 22412157]
12. Eckle SB, Birkinshaw RW, Kostenko L, Corbett AJ, McWilliam HE, Reantragoon R, Chen Z, Gherardin NA, Beddoe T, Liu L, Patel O, Meehan B, Fairlie DP, Villadangos JA, Godfrey DI, Kjer-Nielsen L, McCluskey J, Rossjohn J. A molecular basis underpinning the T cell receptor heterogeneity of mucosal-associated invariant T cells. The Journal of experimental medicine. 2014; 211:1585–1600. [PubMed: 25049336]
13. Martin E, Treiner E, Duban L, Guerri L, Laude H, Toly C, Premel V, Devys A, Moura IC, Tilloy F, Cherif S, Vera G, Latour S, Soudais C, Lantz O. Stepwise development of MAIT cells in mouse and human. PLoS Biol. 2009; 7:e54. [PubMed: 19278296]
14. Okamoto N, Kanie O, Huang YY, Fujii R, Watanabe H, Shimamura M. Synthetic alpha-mannosyl ceramide as a potent stimulant for an NKT cell repertoire bearing the invariant Valpha19-Jalpha26 TCR alpha chain. Chemistry & biology. 2005; 12:677–683. [PubMed: 15975513]
15. Gold MC, McLaren JE, Reistetter JA, Smyk-Pearson S, Ladell K, Swarbrick GM, Yu YY, Hansen TH, Lund O, Nielsen M, Gerritsen B, Kesmir C, Miles JJ, Lewinsohn DA, Price DA, Lewinsohn DM. MR1-restricted MAIT cells display ligand discrimination and pathogen selectivity through distinct T cell receptor usage. The Journal of experimental medicine. 2014; 211:1601–1610. [PubMed: 25049333]
16. Greenaway HY, Ng B, Price DA, Douek DC, Davenport MP, Venturi V. NKT and MAIT invariant TCRalpha sequences can be produced efficiently by VJ gene recombination. Immunobiology. 2013; 218:213–224. [PubMed: 22647874]
17. Riegert P, Wanner V, Bahram S. Genomics, isoforms, expression, and phylogeny of the MHC class I-related MR1 gene. J Immunol. 1998; 161:4066–4077. [PubMed: 9780177]
18. Huang S, Martin E, Kim S, Yu L, Soudais C, Fremont DH, Lantz O, Hansen TH. MR1 antigen presentation to mucosal-associated invariant T cells was highly conserved in evolution. Proc Natl Acad Sci U S A. 2009; 106:8290–8295. [PubMed: 19416870]
19. Gold MC, Cerri S, Smyk-Pearson S, Cansler ME, Vogt TM, Delepine J, Winata E, Swarbrick GM, Chua WJ, Yu YY, Lantz O, Cook MS, Null MD, Jacoby DB, Harriff MJ, Lewinsohn DA, Hansen TH, Lewinsohn DM. Human mucosal associated invariant T cells detect bacterially infected cells. PLoS Biol. 2010; 8:e1000407. [PubMed: 20613858]
20. Le Bourhis L, Martin E, Peguillet I, Guihot A, Froux N, Core M, Levy E, Dusseaux M, Meyssonnier V, Premel V, Ngo C, Riteau B, Duban L, Robert D, Huang S, Rottman M, Soudais C, Lantz O. Antimicrobial activity of mucosal-associated invariant T cells. Nat Immunol. 2010; 11:701–708. [PubMed: 20581831]
21. Billerbeck E, Kang YH, Walker L, Lockstone H, Grafmueller S, Fleming V, Flint J, Willberg CB, Bengsch B, Seigel B, Ramamurthy N, Zitzmann N, Barnes EJ, Thevanayagam J, Bhagwanani A, Leslie A, Oo YH, Kollnberger S, Bowness P, Drognitz O, Adams DH, Blum HE, Thimme R, Klenerman P. Analysis of CD161 expression on human CD8+ T cells defines a distinct functional subset with tissue-homing properties. Proc Natl Acad Sci U S A. 2010; 107:3006–3011. [PubMed: 20133607]
22. Dusseaux M, Martin E, Serriari N, Peguillet I, Premel V, Louis D, Milder M, Le Bourhis L, Soudais C, Treiner E, Lantz O. Human MAIT cells are xenobiotic-resistant, tissue-targeted, CD161hi IL-17-secreting T cells. Blood. 2011; 117:1250–1259. [PubMed: 21084709]
23. Northfield JW, Kasprowicz V, Lucas M, Kersting N, Bengsch B, Kim A, Phillips RE, Walker BD, Thimme R, Lauer G, Klenerman P. CD161 expression on hepatitis C virus-specific CD8+ T cells suggests a distinct pathway of T cell differentiation. Hepatology. 2008; 47:396–406. [PubMed: 18219672]

24. Chua WJ, Truscott SM, Eickhoff CS, Blazevic A, Hoft DF, Hansen TH. Polyclonal mucosa-associated invariant T cells have unique innate functions in bacterial infection. Infect Immun. 2012; 80:3256–3267. [PubMed: 22778103]
25. Kawachi I, Maldonado J, Strader C, Gilfillan S. MR1-restricted V alpha 19i mucosal-associated invariant T cells are innate T cells in the gut lamina propria that provide a rapid and diverse cytokine response. J Immunol. 2006; 176:1618–1627. [PubMed: 16424191]
26. Gold MC, Napier RJ, Lewinsohn DM. MR1-restricted mucosal associated invariant T (MAIT) cells in the immune response to Mycobacterium tuberculosis. Immunological reviews. 2015; 264:154–166. [PubMed: 25703558]
27. Cosgrove C, Ussher JE, Rauch A, Gartner K, Kurioka A, Huhn MH, Adelmann K, Kang YH, Fergusson JR, Simmonds P, Goulder P, Hansen TH, Fox J, Gunthard HF, Khanna N, Powrie F, Steel A, Gazzard B, Phillips RE, Frater J, Uhlig H, Klenerman P. Early and nonreversible decrease of CD161++/MAIT cells in HIV infection. Blood. 2013; 121:951–961. [PubMed: 23255555]
28. Leeansyah E, Ganesh A, Quigley MF, Sonnerborg A, Andersson J, Hunt PW, Somsouk M, Deeks SG, Martin JN, Moll M, Shacklett BL, Sandberg JK. Activation, exhaustion, and persistent decline of the antimicrobial MR1-restricted MAIT-cell population in chronic HIV-1 infection. Blood. 2013; 121:1124–1135. [PubMed: 23243281]
29. Wong EB, Akilimali NA, Govender P, Sullivan ZA, Cosgrove C, Pillay M, Lewinsohn DM, Bishai WR, Walker BD, Ndung'u T, Klenerman P, Kasprowicz VO. Low Levels of Peripheral CD161+ +CD8+ Mucosal Associated Invariant T (MAIT) Cells Are Found in HIV and HIV/TB Co-Infection. PloS one. 2013; 8:e83474. [PubMed: 24391773]
30. Fernandez CS, Amarasena T, Kelleher AD, Rossjohn J, McCluskey J, Godfrey DI, Kent SJ. MAIT cells are depleted early but retain functional cytokine expression in HIV infection. Immunology and cell biology. 2015; 93:177–188. [PubMed: 25348935]
31. Miyazaki Y, Miyake S, Chiba A, Lantz O, Yamamura T. Mucosal-associated invariant T cells regulate Th1 response in multiple sclerosis. International immunology. 2011; 23:529–535. [PubMed: 21712423]
32. Annibali V, Ristori G, Angelini DF, Serafini B, Mechelli R, Cannoni S, Romano S, Paolillo A, Abderrahim H, Diamantini A, Borsellino G, Aloisi F, Battistini L, Salvetti M. CD161(high)CD8+T cells bear pathogenetic potential in multiple sclerosis. Brain: a journal of neurology. 2011; 134:542–554. [PubMed: 21216829]
33. Serriari NE, Eoche M, Lamotte L, Lion J, Fumery M, Marcelo P, Chatelain D, Barre A, Nguyen-Khac E, Lantz O, Dupas JL, Treiner E. Innate mucosal-associated invariant T (MAIT) cells are activated in inflammatory bowel diseases. Clinical and experimental immunology. 2014; 176:266–274. [PubMed: 24450998]
34. Magalhaes I, Pingris K, Poitou C, Bessoles S, Venteclef N, Kiaf B, Beaudoin L, Da Silva J, Allatif O, Rossjohn J, Kjer-Nielsen L, McCluskey J, Ledoux S, Genser L, Torcivia A, Soudais C, Lantz O, Boitard C, Aron-Wisnewsky J, Larger E, Clement K, Lehuen A. Mucosal-associated invariant T cell alterations in obese and type 2 diabetic patients. The Journal of clinical investigation. 2015
35. Treiner E, Duban L, Bahram S, Radosavljevic M, Wanner V, Tilloy F, Affaticati P, Gilfillan S, Lantz O. Selection of evolutionarily conserved mucosal-associated invariant T cells by MR1. Nature. 2003; 422:164–169. [PubMed: 12634786]
36. Georgel P, Radosavljevic M, Macquin C, Bahram S. The non-conventional MHC class I MR1 molecule controls infection by Klebsiella pneumoniae in mice. Molecular immunology. 2011; 48:769–775. [PubMed: 21190736]
37. Meierovics A, Yankelevich WJ, Cowley SC. MAIT cells are critical for optimal mucosal immune responses during in vivo pulmonary bacterial infection. Proc Natl Acad Sci U S A. 2013; 110:E3119–E3128. [PubMed: 23898209]
38. Croxford JL, Miyake S, Huang YY, Shimamura M, Yamamura T. Invariant V(alpha)19i T cells regulate autoimmune inflammation. Nat Immunol. 2006; 7:987–994. [PubMed: 16878136]
39. Walker LJ, Kang YH, Smith MO, Tharmalingham H, Ramamurthy N, Fleming VM, Sahgal N, Leslie A, Oo Y, Geremia A, Scriba TJ, Hanekom WA, Lauer GM, Lantz O, Adams DH, Powrie F, Barnes E, Klenerman P. Human MAIT and CD8alphaalpha cells develop from a pool of type-17 precommitted CD8+ T cells. Blood. 2012; 119:422–433. [PubMed: 22086415]

40. Perarnau B, Saron MF, Reina San Martin B, Bervas N, Ong H, Soloski MJ, Smith AG, Ure JM, Gairin JE, Lemonnier FA. Single H2Kb, H2Db and double H2KbDb knockout mice: peripheral CD8+ T cell repertoire and anti-lymphocytic choriomeningitis virus cytolytic responses. European journal of immunology. 1999; 29:1243–1252. [PubMed: 10229092]
41. Fang X, Du P, Liu Y, Tang J. Efficient isolation of mouse liver NKT cells by perfusion. PloS one. 2010; 5:e10288. [PubMed: 20422018]
42. Huang S, Gilfillan S, Cella M, Miley MJ, Lantz O, Lybarger L, Fremont DH, Hansen TH. Evidence for MR1 antigen presentation to mucosal-associated invariant T cells. J Biol Chem. 2005; 280:21183–21193. [PubMed: 15802267]
43. Huang S, Gilfillan S, Kim S, Thompson B, Wang X, Sant AJ, Fremont DH, Lantz O, Hansen TH. MR1 uses an endocytic pathway to activate mucosal-associated invariant T cells. The Journal of experimental medicine. 2008; 205:1201–1211. [PubMed: 18443227]
44. Miley MJ, Truscott SM, Yu YY, Gilfillan S, Fremont DH, Hansen TH, Lybarger L. Biochemical features of the MHC-related protein 1 consistent with an immunological function. J Immunol. 2003; 170:6090–6098. [PubMed: 12794138]
45. Worku S, Hoft DF. Differential effects of control and antigen-specific T cells on intracellular mycobacterial growth. Infect Immun. 2003; 71:1763–1773. [PubMed: 12654790]
46. Godfrey DI, Masciantonio M, Tucek CL, Malin MA, Boyd RL, Hugo P. Thymic shared antigen-1. A novel thymocyte marker discriminating immature from mature thymocyte subsets. J Immunol. 1992; 148:2006–2011. [PubMed: 1531995]
47. Lepore M, Kalinicenko A, Colone A, Paleja B, Singhal A, Tschumi A, Lee B, Poidinger M, Zolezzi F, Quagliata L, Sander P, Newell E, Bertoletti A, Terracciano L, De Libero G, Mori L. Parallel T-cell cloning and deep sequencing of human MAIT cells reveal stable oligoclonal TCRbeta repertoire. Nature communications. 2014; 5:3866.
48. Baldwin TA, Sandau MM, Jameson SC, Hogquist KA. The timing of TCR alpha expression critically influences T cell development and selection. The Journal of experimental medicine. 2005; 202:111–121. [PubMed: 15998791]
49. Huang CY, Kanagawa O. Impact of early expression of TCR alpha chain on thymocyte development. European journal of immunology. 2004; 34:1532–1541. [PubMed: 15162422]
50. Ussher JE, Bilton M, Attwod E, Shadwell J, Richardson R, de Lara C, Mettke E, Kurioka A, Hansen TH, Klenerman P, Willberg CB. CD161 CD8 T cells, including the MAIT cell subset, are specifically activated by IL-12+IL-18 in a TCR-independent manner. European journal of immunology. 2013
51. Fehniger TA, Shah MH, Turner MJ, VanDeusen JB, Whitman SP, Cooper MA, Suzuki K, Wechser M, Goodsaid F, Caligiuri MA. Differential cytokine and chemokine gene expression by human NK cells following activation with IL-18 or IL-15 in combination with IL-12: implications for the innate immune response. J Immunol. 1999; 162:4511–4520. [PubMed: 10201989]
52. Velazquez P, Cameron TO, Kinjo Y, Nagarajan N, Kronenberg M, Dustin ML. Cutting edge: activation by innate cytokines or microbial antigens can cause arrest of natural killer T cell patrolling of liver sinusoids. J Immunol. 2008; 180:2024–2028. [PubMed: 18250405]
53. Tomura M, Maruo S, Mu J, Zhou XY, Ahn HJ, Hamaoka T, Okamura H, Nakanishi K, Clark S, Kurimoto M, Fujiwara H. Differential capacities of CD4+, CD8+, and CD4−CD8− T cell subsets to express IL-18 receptor and produce IFN-gamma in response to IL-18. J Immunol. 1998; 160:3759–3765. [PubMed: 9558078]
54. Slight SR, Khader SA. Chemokines shape the immune responses to tuberculosis. Cytokine & growth factor reviews. 2013; 24:105–113. [PubMed: 23168132]
55. Feng CG, Britton WJ, Palendira U, Groat NL, Briscoe H, Bean AG. Up-regulation of VCAM-1 and differential expansion of beta integrin-expressing T lymphocytes are associated with immunity to pulmonary Mycobacterium tuberculosis infection. J Immunol. 2000; 164:4853–4860. [PubMed: 10779794]
56. Peters W, Ernst JD. Mechanisms of cell recruitment in the immune response to Mycobacterium tuberculosis. Microbes Infect. 2003; 5:151–158. [PubMed: 12650773]

57. Tang XZ, Jo J, Tan AT, Sandalova E, Chia A, Tan KC, Lee KH, Gehring AJ, De Libero G, Bertoletti A. IL-7 licenses activation of human liver intrasinusoidal mucosal-associated invariant T cells. J Immunol. 2013; 190:3142–3152. [PubMed: 23447689]
58. Seach N, Guerri L, Le Bourhis L, Mburu Y, Cui Y, Bessoles S, Soudais C, Lantz O. Double positive thymocytes select mucosal-associated invariant T cells. J Immunol. 2013; 191:6002–6009. [PubMed: 24244014]
59. Leeansyah E, Loh L, Nixon DF, Sandberg JK. Acquisition of innate-like microbial reactivity in mucosal tissues during human fetal MAIT-cell development. Nature communications. 2014; 5:3143.
60. Le Bourhis L, Dusseaux M, Bohineust A, Bessoles S, Martin E, Premel V, Core M, Sleurs D, Serriari NE, Treiner E, Hivroz C, Sansonetti P, Gougeon ML, Soudais C, Lantz O. MAIT Cells Detect and Efficiently Lyse Bacterially-Infected Epithelial Cells. PLoS pathogens. 2013; 9:e1003681. [PubMed: 24130485]
61. Wei DG, Curran SA, Savage PB, Teyton L, Bendelac A. Mechanisms imposing the Vbeta bias of Valpha14 natural killer T cells and consequences for microbial glycolipid recognition. The Journal of experimental medicine. 2006; 203:1197–1207. [PubMed: 16651387]
62. Rossjohn J, Pellicci DG, Patel O, Gapin L, Godfrey DI. Recognition of CD1d-restricted antigens by natural killer T cells. Nature reviews. Immunology. 2012; 12:845–857.
63. Lopez-Sagaseta J, Dulberger CL, Crooks JE, Parks CD, Luoma AM, McFedries A, Van Rhijn I, Saghatelian A, Adams EJ. The molecular basis for Mucosal-Associated Invariant T cell recognition of MR1 proteins. Proc Natl Acad Sci U S A. 2013; 110:E1771–1778. [PubMed: 23613577]
64. Eckle SB, Turner SJ, Rossjohn J, McCluskey J. Predisposed alphabeta T cell antigen receptor recognition of MHC and MHC-I like molecules? Current opinion in immunology. 2013; 25:653–659. [PubMed: 23993410]
65. Shimamura M, Huang YY. Presence of a novel subset of NKT cells bearing an invariant V(alpha)19.1-J(alpha)26 TCR alpha chain. FEBS letters. 2002; 516:97–100. [PubMed: 11959111]
66. Arase H, Arase N, Saito T. Interferon gamma production by natural killer (NK) cells and NK1.1+ T cells upon NKR-P1 cross-linking. The Journal of experimental medicine. 1996; 183:2391–2396. [PubMed: 8642351]
67. Arase N, Arase H, Park SY, Ohno H, Ra C, Saito T. Association with FcRgamma is essential for activation signal through NKR-P1 (CD161) in natural killer (NK) cells and NK1.1+ T cells. The Journal of experimental medicine. 1997; 186:1957–1963. [PubMed: 9396764]
68. Chambers WH, Vujanovic NL, DeLeo AB, Olszowy MW, Herberman RB, Hiserodt JC. Monoclonal antibody to a triggering structure expressed on rat natural killer cells and adherent lymphokine-activated killer cells. The Journal of experimental medicine. 1989; 169:1373–1389. [PubMed: 2466943]
69. Giorda R, Rudert WA, Vavassori C, Chambers WH, Hiserodt JC, Trucco M. NKR-P1, a signal transduction molecule on natural killer cells. Science. 1990; 249:1298–1300. [PubMed: 2399464]
70. Bartel Y, Bauer B, Steinle A. Modulation of NK Cell Function by Genetically Coupled C-Type Lectin-Like Receptor/Ligand Pairs Encoded in the Human Natural Killer Gene Complex. Frontiers in immunology. 2013; 4:362. [PubMed: 24223577]
71. Kadioglu A, De Filippo K, Bangert M, Fernandes VE, Richards L, Jones K, Andrew PW, Hogg N. The integrins Mac-1 and alpha4beta1 perform crucial roles in neutrophil and T cell recruitment to lungs during Streptococcus pneumoniae infection. J Immunol. 2011; 186:5907–5915. [PubMed: 21460207]
72. Walrath JR, Silver RF. The alpha4beta1 integrin in localization of Mycobacterium tuberculosis-specific T helper type 1 cells to the human lung. American journal of respiratory cell and molecular biology. 2011; 45:24–30. [PubMed: 20724551]
73. Rabin RL, Park MK, Liao F, Swofford R, Stephany D, Farber JM. Chemokine receptor responses on T cells are achieved through regulation of both receptor expression and signaling. J Immunol. 1999; 162:3840–3850. [PubMed: 10201901]
74. Sallusto F, Lanzavecchia A, Mackay CR. Chemokines and chemokine receptors in T-cell priming and Th1/Th2-mediated responses. Immunol Today. 1998; 19:568–574. [PubMed: 9864948]

75. Kohlmeier JE, Cookenham T, Miller SC, Roberts AD, Christensen JP, Thomsen AR, Woodland DL. CXCR3 directs antigen-specific effector CD4+ T cell migration to the lung during parainfluenza virus infection. J Immunol. 2009; 183:4378–4384. [PubMed: 19734208]

76. Farber JM. Mig and IP-10: CXC chemokines that target lymphocytes. Journal of leukocyte biology. 1997; 61:246–257. [PubMed: 9060447]

77. Lu B, Humbles A, Bota D, Gerard C, Moser B, Soler D, Luster AD, Gerard NP. Structure and function of the murine chemokine receptor CXCR3. European journal of immunology. 1999; 29:3804–3812. [PubMed: 10556837]

78. Groom JR, Luster AD. CXCR3 ligands: redundant, collaborative and antagonistic functions. Immunology and cell biology. 2011; 89:207–215. [PubMed: 21221121]

79. Lim J, Derrick SC, Kolibab K, Yang AL, Porcelli S, Jacobs WR, Morris SL. Early pulmonary cytokine and chemokine responses in mice immunized with three different vaccines against Mycobacterium tuberculosis determined by PCR array. Clinical and vaccine immunology: CVI. 2009; 16:122–126. [PubMed: 19038785]

80. Sauty A, Dziejman M, Taha RA, Iarossi AS, Neote K, Garcia-Zepeda EA, Hamid Q, Luster AD. The T cell-specific CXC chemokines IP-10, Mig, and I-TAC are expressed by activated human bronchial epithelial cells. J Immunol. 1999; 162:3549–3558. [PubMed: 10092813]

81. Barouch DH, Santra S, Schmitz JE, Kuroda MJ, Fu TM, Wagner W, Bilska M, Craiu A, Zheng XX, Krivulka GR, Beaudry K, Lifton MA, Nickerson CE, Trigona WL, Punt K, Freed DC, Guan L, Dubey S, Casimiro D, Simon A, Davies ME, Chastain M, Strom TB, Gelman RS, Montefiori DC, Lewis MG, Emini EA, Shiver JW, Letvin NL. Control of viremia and prevention of clinical AIDS in rhesus monkeys by cytokine-augmented DNA vaccination. Science. 2000; 290:486–492. [PubMed: 11039923]

82. Morrow MP, Pankhong P, Laddy DJ, Schoenly KA, Yan J, Cisper N, Weiner DB. Comparative ability of IL-12 and IL-28B to regulate Treg populations and enhance adaptive cellular immunity. Blood. 2009; 113:5868–5877. [PubMed: 19304955]

83. Kalams SA, Parker S, Jin X, Elizaga M, Metch B, Wang M, Hural J, Lubeck M, Eldridge J, Cardinali M, Blattner WA, Sobieszczyk M, Suriyanon V, Kalichman A, Weiner DB, Baden LR, Network NHVT. Safety and immunogenicity of an HIV-1 gag DNA vaccine with or without IL-12 and/or IL-15 plasmid cytokine adjuvant in healthy, HIV-1 uninfected adults. PloS one. 2012; 7:e29231. [PubMed: 22242162]

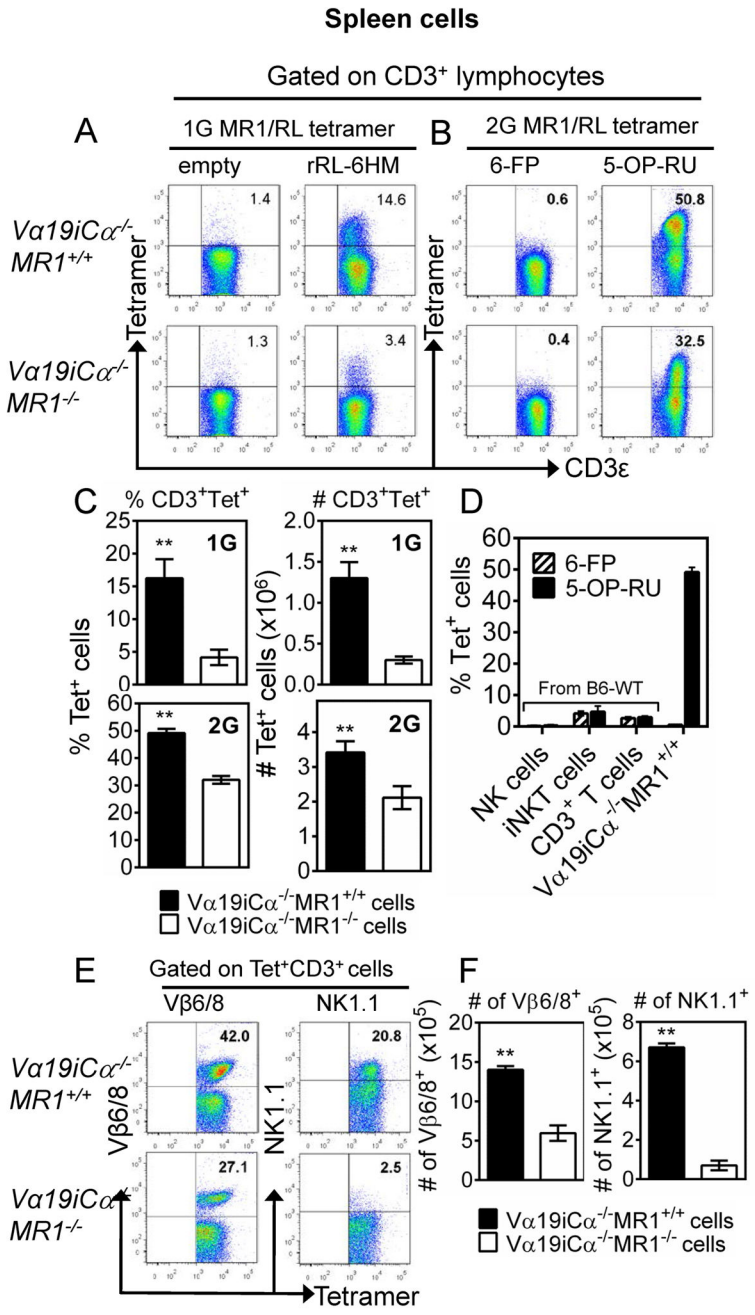

FIGURE 1.

Mouse MR1/RL tetramers stain phenotypically diverse subsets of CD3$^+$ cells in *Vα19i* Tg mice on both MR1$^{+/+}$ and MR1$^{-/-}$ genetic background. Purified splenic T cells from antigen-naïve *Vα19iCα*$^{-/-}$*MR1*$^{+/+}$ or *Vα19iCα*$^{-/-}$*MR1*$^{-/-}$ mice were stained with anti-mouse CD3ε, CD4, CD8α, NK1.1 (clone PK136), Vβ6/8.1-2 TCR and mouse MR1 tetramers, and analysed by flow cytometry. (**A**) Representative FACS plots of CD3ε (X-axis) vs. tetramer (Y-axis) gated on splenic CD3$^+$ lymphocyte population for CD3$^+$ T cells stained with first generation (1G) mouse MR1 tetramers loaded with “empty” as negative control or loaded with antigenic rRL-6HM. (**B**) Representative FACS plots of splenic CD3$^+$

T cells stained with second generation (2G) mouse MR1 tetramers, loaded with non-antigenic 6-FP as negative control or loaded with antigenic 5-OP-RU. The percentages of stained cells are indicated. (**C, top panel**) Percentages (left bar graph) and absolute numbers (AN) (right bar graph) of 1G tetramer$^+$ CD3$^+$ cells in *Va19iCa*$^{-/-}$*MR1*$^{+/+}$ or *Va19iCa*$^{-/-}$*MR1*$^{-/-}$ mice. (**C, bottom panel**) Percentages (left bar graph) and AN (right bar graph) of 2G tetramer$^+$ CD3$^+$ cells in *Va19iCa*$^{-/-}$*MR1*$^{+/+}$ or *Va19iCa*$^{-/-}$*MR1*$^{-/-}$ mice. (**D**) Shown is staining of purified splenic NK, type I NKT and bulk T cells from non-transgenic wild type B6 mice with murine MR1–6-FP or MR1–5-OP-RU tetramers, compared with *Va19iCa*$^{-/-}$*MR1*$^{+/+}$ T cells. (**E**) Representative FACS plots of percentage Vβ6/8$^+$ (left panel) or NK1.1 (right panel) of 2G tetramer$^+$CD3$^+$ T cells in *Va19iCa*$^{-/-}$*MR1*$^{+/+}$ or *Va19iCa*$^{-/-}$*MR1*$^{-/-}$ mice. (**F**) AN of Vβ6/8$^+$ (right panel) or NK1.1$^+$ (right panel) of 2G tetramer$^+$ CD3$^+$ T cells in *Va19iCa*$^{-/-}$*MR1*$^{+/+}$ or *Va19iCa*$^{-/-}$*MR1*$^{-/-}$ mice. Data shown are representative of three separate experiments. *P* values are obtained by Mann-Whitney U-tests (n = 5/group) (**$p<0.01$).

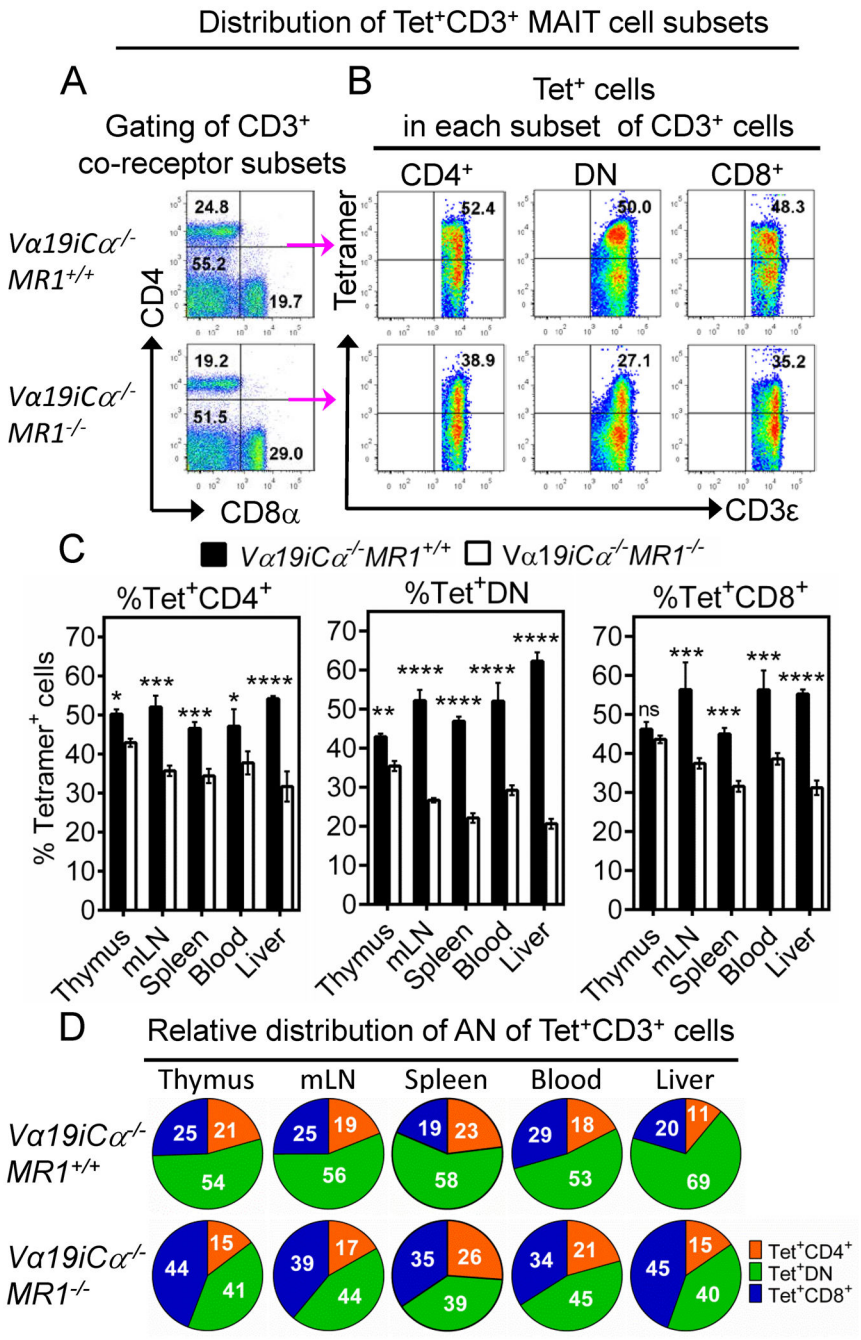

FIGURE 2.

Frequency of CD3$^+$ tetramer$^+$ MAIT cell subsets in the thymus (CD3^{high} thymocytes), mLN, spleen, blood and liver in *Vα19iCα*$^{-/-}$*MR1*$^{+/+}$ or *Vα19iCα*$^{-/-}$*MR1*$^{-/-}$ mice. (**A**) Representative FACS plots of CD4 vs. CD8α gated on CD3$^+$ lymphocyte population for CD4$^-$CD8$^-$ (DN), CD4$^+$CD8$^-$ and CD4$^-$CD8$^+$ co-receptor CD3$^+$ subsets in the spleen of *Vα19iCα*$^{-/-}$*MR1*$^{+/+}$ or *Vα19iCα*$^{-/-}$*MR1*$^{-/-}$ mice. (**B**) Staining of tetramer$^+$ cells among CD4$^+$ (left plots), DN (centre plots) or CD8$^+$ (right plots) CD3$^+$ splenocytes from *Vα19iTgMR1*$^{+/+}$ (top panels) or *Vα19iCα*$^{-/-}$*MR1*$^{-/-}$ (bottom panels) mice. (**C**) Percentages

of tetramer^{+} CD4^{+} T cells (left panel), tetramer^{+} DN T cells (middle panel) and tetramer^{+} CD8^{+} T cells (right panel) in the indicated tissues are shown. (**D**) Pie charts comparing the relative distribution of absolute numbers of tetramer^{+} CD3^{+} T cell subsets in the indicated tissues of *Vα19iCα*$^{-/-}$*MR1*$^{+/+}$ (top panel) or *Vα19iCα*$^{-/-}$*MR1*$^{-/-}$ (bottom panel) mice. Data shown are from more than three separate experiments. *P* values (obtained using Mann-Whitney U-test and 2way ANOVA (multiple comparison test)) denote comparison of mean differences ± SEM of % tetramer^{+} cells between *Vα19iCα*$^{-/-}$*MR1*$^{+/+}$ and *Vα19iCα*$^{-/-}$*MR1*$^{-/-}$ mice. *p<0.05; **p<0.01 and ***p<0.001, ****p<0.0001.

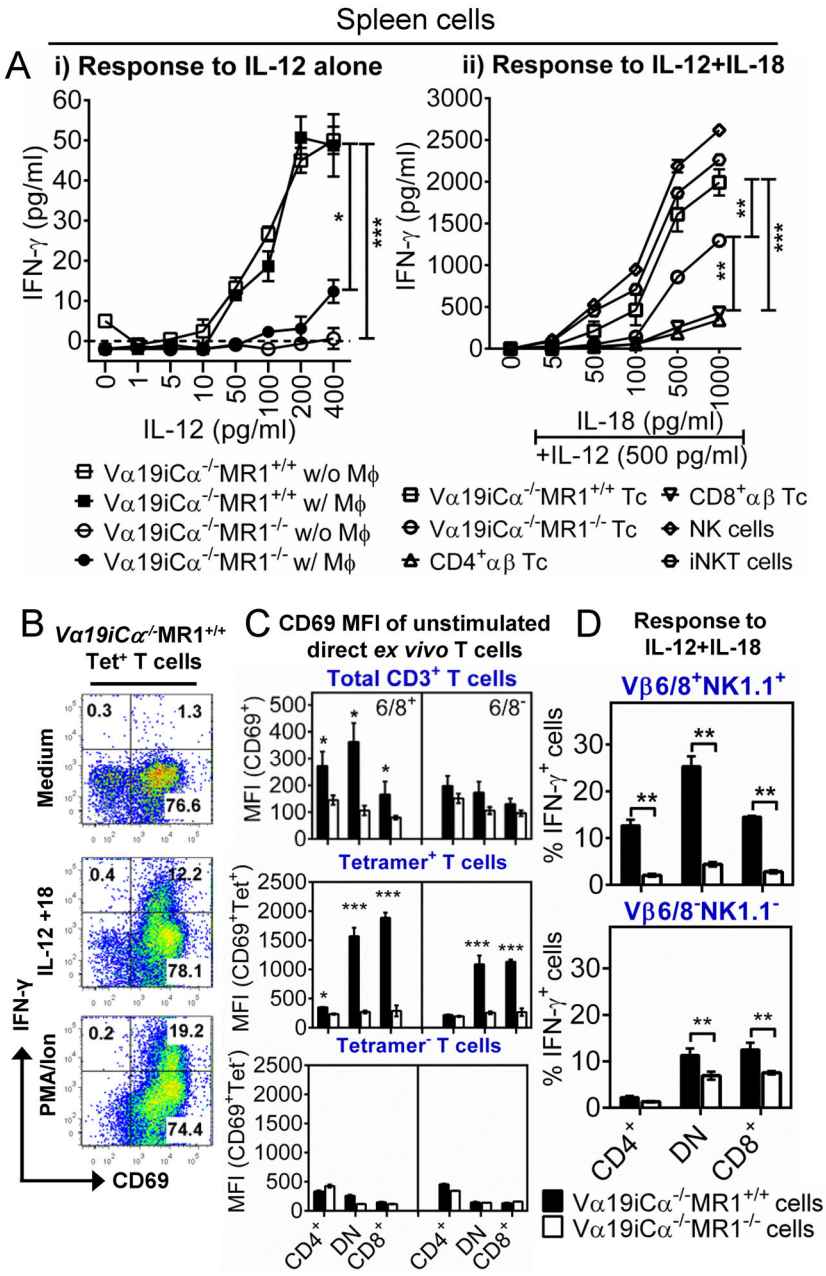

FIGURE 3.

Responsiveness of *Vα19i* transgenic T cells to IL-12 and IL-18 combination. (**A-i**) Splenic T cells from naïve *Vα19iCα*$^{-/-}$*MR1*$^{+/+}$ or *Vα19iCα*$^{-/-}$*MR1*$^{-/-}$ mice were stimulated with indicated doses of IL-12 alone in the presence or absence of BMDMφ (w/Mφ or w/o Mφ, respectively). Data shown are from one of two independent experiments with similar results. (**A-ii**) Splenic T cells (Tc) from naïve *Vα19iCα*$^{-/-}$*MR1*$^{+/+}$ or *Vα19iCα*$^{-/-}$*MR1*$^{-/-}$ mice, conventional CD4^{+} and CD8^{+} αβ T cells, type I NKT (iNKT) and NK cells from naïve B6-WT mice were stimulated with 500 pg/ml IL-12 plus IL-18 (5pg/ml – 1000pg/ml) in the absence of BMDMφ for 24h. IFN-γ in triplicate culture supernatants were determined by ELISA. (**B**) FACS plots showing percentage of intracellular IFN-γ produced by activated

(CD69$^+$) sort-purified tetramer$^+$ T cells after 24h stimulation with 500 pg/ml IL-12 plus 1000 pg/ml IL-18. Data shown are representative of three experiments with similar results. (**C**) Data from two separate experiments showing mean fluorescent intensities for CD69 staining on Vβ6/8$^+$ and Vβ6/8$^-$ bulk *Vα19i* T cells (top panel), FACS sorted tetramer$^+$ cells (middle panel) or FACS sorted tetramer$^-$ cells (bottom panel), from naïve *Vα19iCα*$^{-/-}$*MR1*$^{+/+}$ or *Vα19iCα*$^{-/-}$*MR1*$^{-/-}$ mice. (**D**) Shown is percentage of intracellular IFN-γ produced by tetramer$^+$ Vβ6/8$^+$NK1.1$^+$ cells (top panel) or tetramer$^+$ Vβ6/8$^-$NK1.1$^-$ cells (bottom panel) after 24h stimulation with 500 pg/ml IL-12 plus 1000 pg/ml IL-18. Tetramer$^+$ Vβ6/8$^+$NK1.1$^+$ cells are the best responder subset to IL-12 plus IL-18, and the response depends on the presence of MR1 during development. *P* values (unpaired 2-tailed *t* test) in comparison are *$p<0.05$; **$p<0.01$ and ***$p<0.001$.

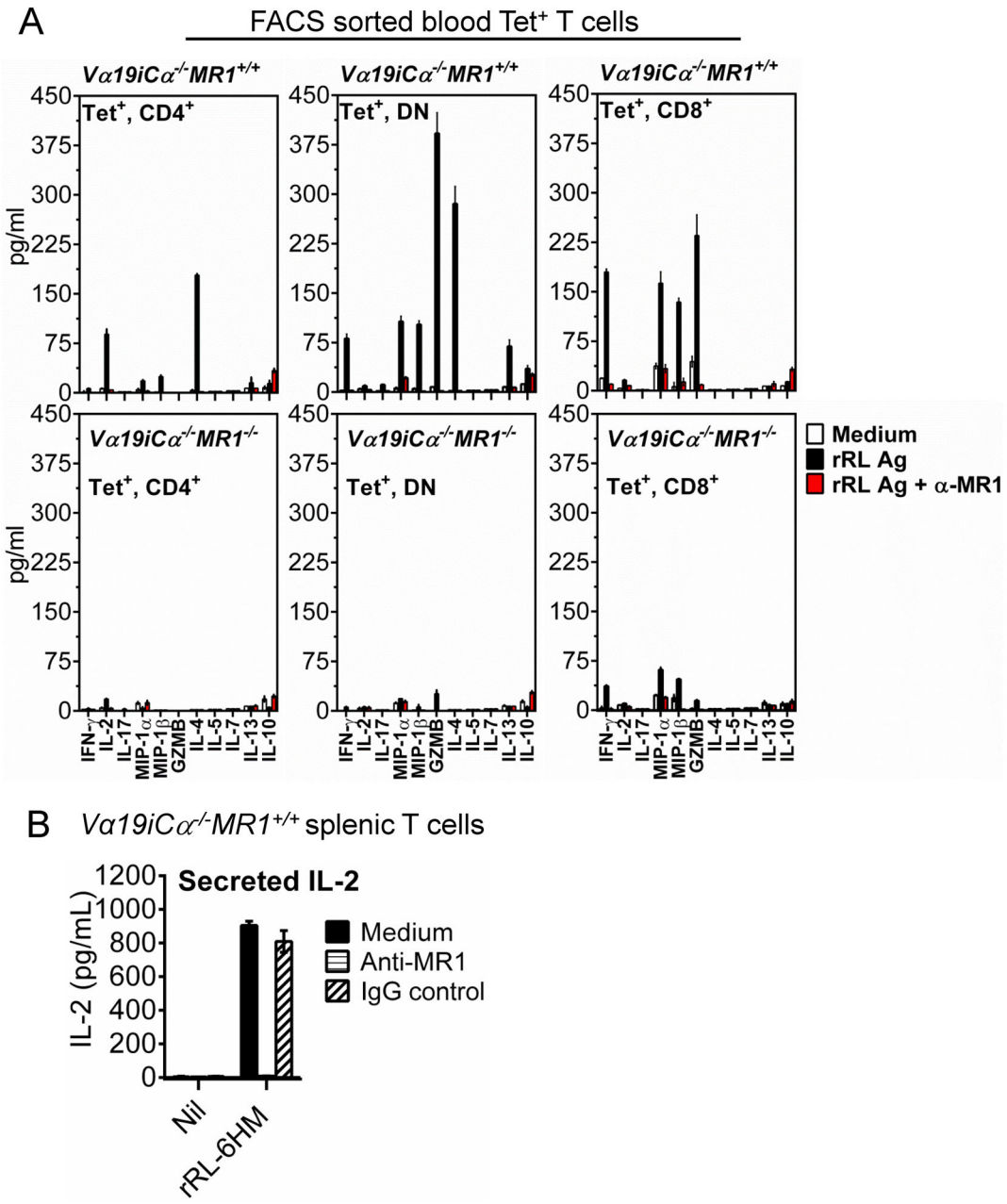

FIGURE 4.

Vα19iCα$^{-/-}$*MR1*$^{+/+}$ T cells respond to RL antigen better than *Vα19iTgMR1*$^{-/-}$ T cells. (A) Peripheral blood mononuclear cells (PBMC) from twenty two (22) *Vα19iCα*$^{-/-}$*MR1*$^{+/+}$ (upper panel) or *Vα19iCα*$^{-/-}$*MR1*$^{-/-}$ (bottom panel) mice were stained with antibodies specific for CD3ε, CD4, CD8α and MR1/RL tetramer, and tetramer^{+} cells sorted by FACS. Sorted tetramer^{+} cells were rested overnight in medium and then co-cultured in triplicates (2.5×10^3 cells/well) with CH27-mMR1 APCs (500 cells/well) along with medium alone, rRL-6HM (rRL) antigen or rRL Ag plus 10μg/ml anti-MR1 for 60h at 37°C. The indicated cytokines, chemokines and GZMB were measured in supernatants using Multiplex bead array assays according to manufacturer's instructions (Milliplex MAP Assays from EMD

Millipore). Tetramer^{+} *Vα19iCα*$^{-/-}$*MR1*$^{+/+}$ T cells are functionally capable MAIT cells. (B) Anti-MR1 antibody, but not mouse IgG isotype control, specifically blocks Ag presentation by APC. Shown is the activation of *Vα19iCα*$^{-/-}$*MR1*$^{+/+}$ T cells by rRL-6HM Ag. Purified MR1$^{+/+}$ splenic *Vα19i* Tg T cells (2×10^5/well) were co-cultured with CH27-mMR1 APCs (4×10^4 cells/well) along with nothing (Nil) or 76.2 μM (final concentration) rRL-6HM in triplicate wells. APCs and Tg T cells were co-cultured overnight (24h) at 37°C in the absence or presence of anti-MR1 blocking antibodies or mouse IgG isotype control. MAIT cell activation was determined by IL-2 secretion using ELISA.

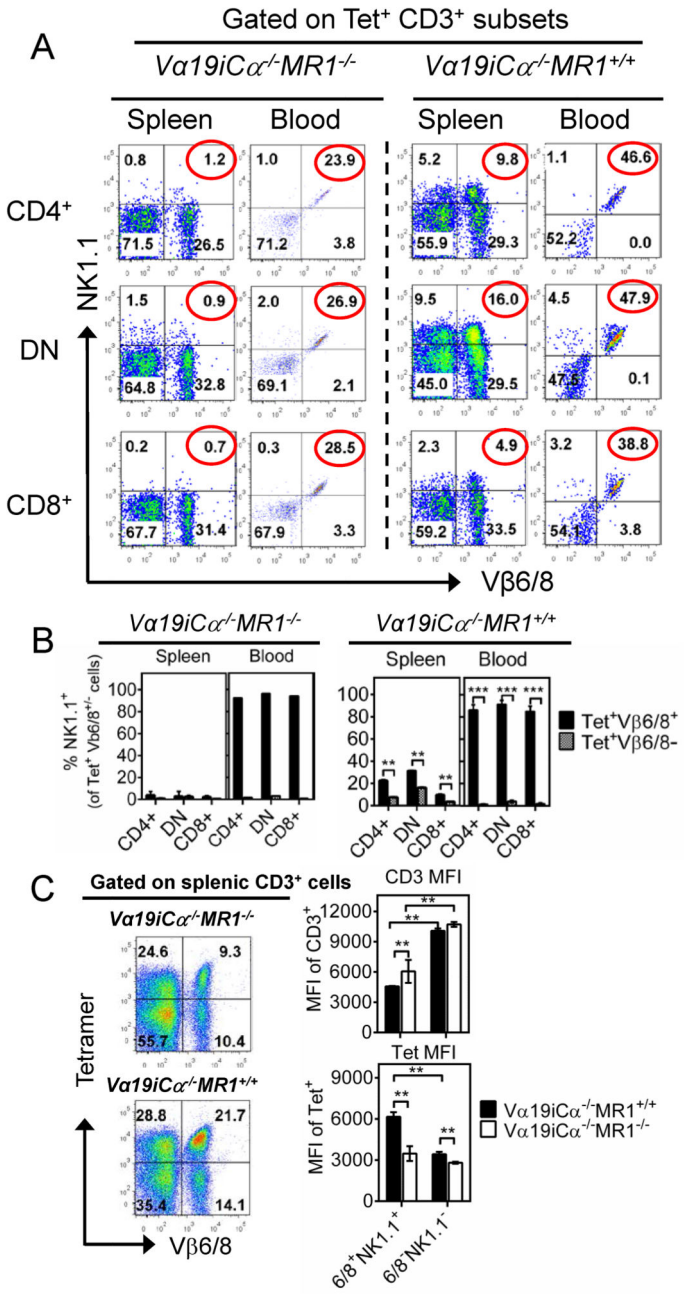

FIGURE 5.

Peripheral expansion of Vβ6/8$^+$NK1.1$^+$ population of tetramer$^+$ CD3$^+$ T cells in *Vα19i* Tg mice. (**A**) Shows surface Vβ6/8.1-2 (X-axis) and NK1.1 (Y-axis) expression on tetramer$^+$ CD4$^+$ (*top plots*), DN (*middle plots*) or CD8$^+$ (*bottom plots*) T cells in spleen and blood from uninfected *Vα19iCα*$^{-/-}$*MR1*$^{-/-}$ (left panel) *Vα19iCα*$^{-/-}$*MR1*$^{+/+}$ (right panel) mice. Numbers in the upper right quadrants are NK1.1$^+$ and Vβ6/8.1-2$^+$ cells. (**B**) Increasing enrichment of tetramer$^+$ NK1.1 lineage in Vβ6/8$^+$ cells more than in Vβ6/8$^-$ subset from spleen to blood. (**C**) *Vα19i* Tg cells developing with MR1 have higher affinity for MR1/RL complexes. Shown in the left panel are Vβ6/8 (X-axis) vs. tetramer (Y-axis) FACS plots of

splenic CD3$^+$ MAIT cells from *Vα19iCα*$^{-/-}$*MR1*$^{-/-}$or *Vα19iCα*$^{-/-}$*MR1*$^{+/+}$ mice. Shown in the right panel are mean fluorescence intensities of CD3ε (top bar graph) and tetramer (bottom bar graph) staining of splenic tetramer$^+$ Vβ6/8$^+$NK1.1$^+$ or Vβ6/8$^-$NK1.1$^-$ CD3$^+$ T cells from *Vα19iCα*$^{-/-}$*MR1*$^{+/+}$ or *Vα19iCα*$^{-/-}$*MR1*$^{-/-}$ mice. Despite lower CD3 expression, *Vα19i* Tg T cells from MR1$^{+/+}$ mice display higher affinity for MR1/RL tetramers than *Vα19i* Tg cells from MR1$^{-/-}$ mice. Furthermore, tetramer$^+$ CD3$^+$ MAIT cells expressing both Vβ6/8 and NK1.1 in *Vα19i* Tg MR1 sufficient mice display the highest affinity for tetramer binding. Data shown are from two separate experiments. *P* values are obtained by Mann-Whitney U-tests (n = 5/group) (**p<0.01 and ***p<0.001).

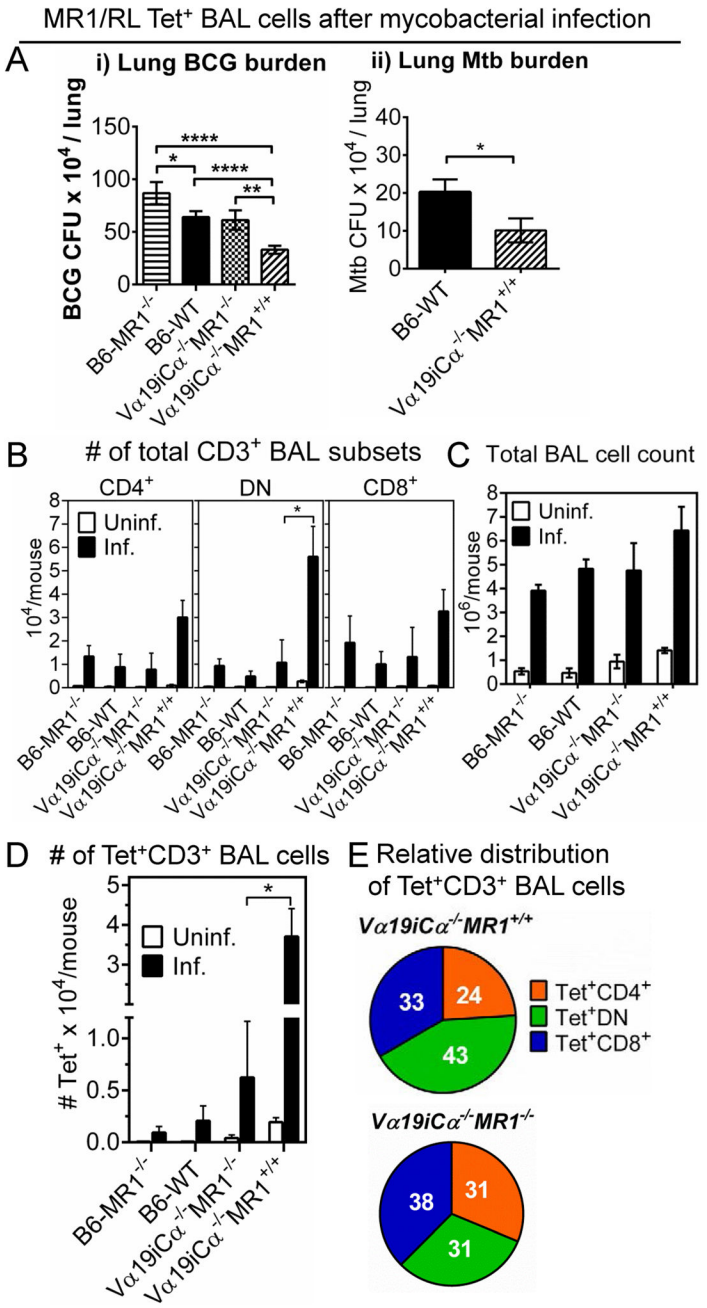

FIGURE 6.

MR1/RL tetramer+ T cells accumulate in the lung during mycobacteria primary infection. Groups of 5 - 11 B6-MR1$^{-/-}$, B6-WT, *Vα19iCα*$^{-/-}$*MR1*$^{-/-}$ or *Vα19iCα*$^{-/-}$*MR1*$^{+/+}$ mice were infected with *M. bovis* BCG Danish or *M. tuberculosis* Erdman as described in the *Materials and Methods*. At day 10 post-infection, BAL fluids collected from uninfected and infected groups were pooled for staining with tetramer and other phenotypic markers. The bacterial burden was determined by CFU plating of lung tissue homogenates. (**A**) Bar graphs showing *M. bovis* BCG Danish (**i**) and *M. tuberculosis* Erdman CFUs (**ii**) in lungs of infected mice. Results are mean ± SEM of mycobacteria CFUs, and are from three

independent experiments. (**B**) Absolute numbers (AN) of BAL $CD3^+$ lymphocytes in uninfected or infected mice. (**C**) Data from three independent experiments showing total leukocyte counts in BAL fluids from uninfected and infected mice. (**D**) Bar graphs showing AN of BAL $tetramer^+$ $CD3^+$ T cells in the indicated mice. (**E**) Pie charts showing relative distribution of absolute numbers of $tetramer^+$ $CD3^+$ MAIT cell subsets in infected $Va19iCa^{-/-}MR1^{+/+}$ (top pie chart) or $Va19iCa^{-/-}MR1^{-/-}$ (bottom pie chart) mice. *P* values were obtained by using Mann Whitney U test (*$p<0.05$; **$p<0.01$, and ****$p<0.0001$).

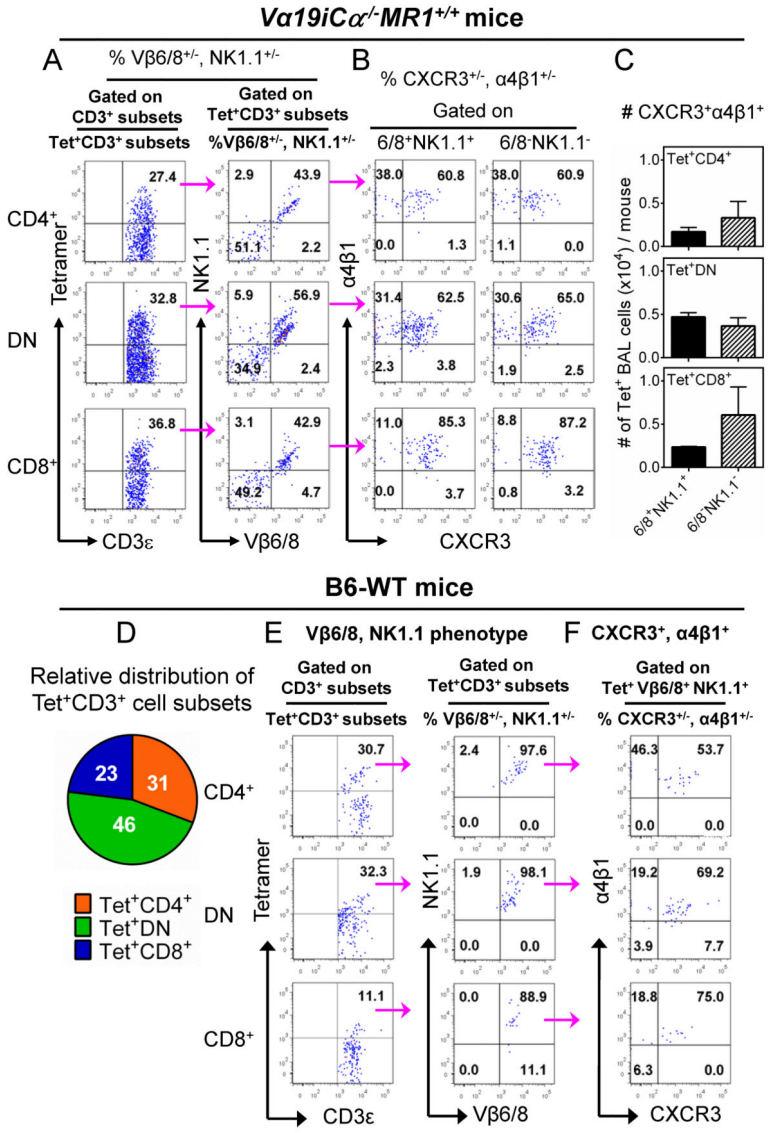

FIGURE 7.

Vβ6/8 and NK1.1 expression by BAL tetramer$^+$ CD3$^+$ MAIT cells in *Vα19iCα*$^{-/-}$*MR1*$^{+/+}$ and B6-WT mice after mycobacterial infection. (**A – C**) Phenotype of tetramer$^+$ CD3$^+$ MAIT cell subsets in BAL fluids from infected *Vα19iCα*$^{-/-}$*MR1*$^{+/+}$ mice. (**A**) (Left column) Representative FACS plots from three separate experiments showing percentages of tetramer$^+$ CD3$^+$ *Vα19i* Tg T cell subsets. The numbers in the upper right quadrants indicate tetramer$^+$ CD4$^+$ (*top plot*), tetramer$^+$ DN (*middle plot*) and tetramer$^+$ CD8$^+$ (*bottom plot*) MAIT cells. (Right column) Representative plots showing Vβ6/8.1-2 (X-axis) and NK1.1 (Y-axis) expression on tetramer$^+$ CD4$^+$ (*top plot*), DN (*middle plot*) or CD8$^+$ (*bottom plot*) MAIT cells. The numbers in the quadrants indicate i) NK1.1$^-$Vβ6/8.1-2$^-$ tetramer$^+$ cells (lower left quadrats), ii) NK1.1$^+$ Vβ6/8.1-2$^-$ tetramer$^+$ cells (upper left quadrats), iii) NK1.1$^+$Vβ6/8.1-2$^+$ tetramer$^+$ cells (upper right quadrats) and iv) NK1.1$^-$ Vβ6/8.1-2$^+$ tetramer$^+$ cells (lower right quadrats). The NK1.1$^-$ Vβ6/8$^-$ tetramer$^+$ and NK1.1$^+$Vβ6/8$^+$ cells were the most predominant subpopulations. (**B**) Representative data from three

separate experiments showing percentage of CXCR3 (X-axis) and α4β1 (Y-axis) expression on NK1.1^{+}Vβ6/8^{+} or NK1.1^{-}Vβ6/8^{-} tetramer^{+} CD4^{+} (*top plots*), DN (*middle plots*) or CD8^{+} (*bottom plots*) MAIT cells in BAL from infected *Vα19iCα*$^{-/-}$*MR1*$^{+/+}$ mice. Numbers in the upper right quadrants are proportions of cells that expressed both CXCR3 and α4β1 integrin. (**C**) Representative data from three separate experiments showing AN of CXCR3 and α4β1-expressing NK1.1^{+}Vβ6/8^{+} or NK1.1^{-} Vβ6/8^{-} tetramer^{+} CD4^{+} (*top bar*), DN (*middle bar*) or CD8^{+} (*bottom bar*) MAIT cells. (**D – F**) Frequency and phenotype of tetramer^{+} CD3^{+} non-Tg MAIT cell subsets in BAL fluids from infected B6-WT mice. (**D**) The pie chart shows the relative distribution of absolute numbers of tetramer^{+} CD3^{+} MAIT cell subsets in the BAL fluids from infected B6-WT mice. (**E**) (Left column) Representative FACS plots showing percentages of tetramer^{+} CD3^{+} MAIT cell subsets. Numbers in the upper right quadrants indicate tetramer^{+} CD4^{+} (*top plot*), tetramer^{+} DN (*middle plot*) and tetramer^{+} CD8^{+} (*bottom plot*) MAIT cells. (Right column) Representative FACS plots showing Vβ6/8 (X-axis) and NK1.1 (Y-axis) expression on tetramer^{+} CD3^{+} MAIT cell subsets. Numbers in the upper right quadrants are proportions of tetramer^{+} cells that expressed both Vβ6/8 and NK1.1, and (**F**) CXCR3 and α4β1 integrin expression on Vβ6/8^{+}NK1.1^{+} tetramer^{+} MAIT cell population in the airways of infected B6-WT mice.

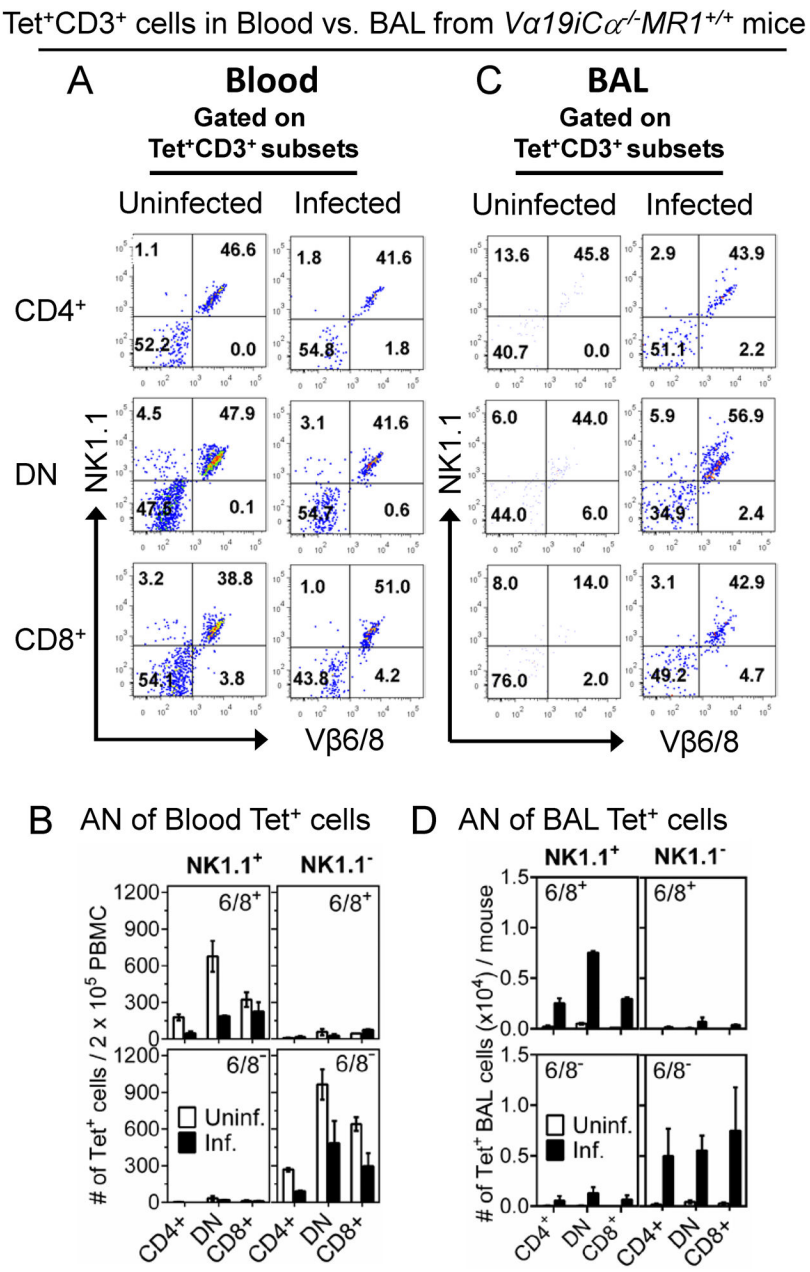

FIGURE 8.

Vβ6/8 and NK1.1 phenotype of *Vα19i* Tg T cells in blood and BAL from uninfected or mycobacterial-infected *Vα19iCα*$^{-/-}$*MR1*$^{+/+}$ mice. *Vα19iCα*$^{-/-}$*MR1*$^{+/+}$ mice were infected with 10^7 CFU/mouse of BCG Danish as described in Fig. 6. At day 10 post-infection peripheral blood T cells were stained with tetramer and a panel of other phenotypic markers and analysed by FACS. (**A**) FACS plots from one of the two separate experiments showing percentages of Vβ6/8.1-2 (X-axis) and NK1.1 (Y-axis) expression on tetramer$^+$ CD4$^+$ (*top plots*), DN (*middle plots*) or CD8$^+$ (*bottom plots*) MAIT cells in blood from uninfected or infected *Vα19iCα*$^{-/-}$*MR1*$^{+/+}$ mice. (**B**) Data from two separate experiments showing number of tetramer$^+$ NK1.1$^+$ or tetramer$^+$ NK1.1$^-$ cells that were either Vβ6/8$^+$ (*top panels*)

or Vβ6/8^{-} (*bottom panel*) cells in blood from uninfected or infected *Vα19iCα*$^{-/-}$*MR1*$^{+/+}$ mice. (**C**) Representative data from one of the three separate experiments showing percentages of Vβ6/8.1-2 and NK1.1 expression on tetramer^{+} CD4^{+} (*top plots*), DN (*middle plots*) or CD8^{+} (*bottom plots*) MAIT cells in BAL from uninfected or infected *Vα19iCα*$^{-/-}$*MR1*$^{+/+}$ mice. (**D**) Data from two separate experiments showing number of tetramer^{+} NK1.1^{+} or tetramer^{+} NK1.1^{-} cells that were either Vβ6/8^{+} (*top panels*) or Vβ6/8^{-} (*bottom panel*) cells in BAL from uninfected or infected *Vα19iCα*$^{-/-}$*MR1*$^{+/+}$ mice.